

The Impact of Anthropogenic Land-Cover Change on the Florida Peninsula Sea Breezes and Warm Season Sensible Weather

CURTIS H. MARSHALL AND ROGER A. PIELKE SR.

Department of Atmospheric Science, Colorado State University, Fort Collins, Colorado

LOUIS T. STEYAERT

EROS Data Center, U.S. Geological Survey, and NASA Goddard Space Flight Center, Greenbelt, Maryland

DEBRA A. WILLARD

U.S. Geological Survey, Reston, Virginia

(Manuscript received 3 October 2002, in final form 13 June 2003)

ABSTRACT

During the twentieth century, the natural landscape of the Florida peninsula was transformed extensively by agriculture, urbanization, and the diversion of surface water features. The purpose of this paper is to present a numerical modeling study in which the possible impacts of this transformation on the warm season climate of the region were investigated. For three separate July–August periods (1973, 1989, and 1994), a pair of simulations was performed with the Regional Atmospheric Modeling System. Within each pair, the simulations differed only in the specification of land-cover class. The two different classes were specified using highly detailed datasets that were constructed to represent pre-1900 natural land cover and 1993 land-use patterns, thus capturing the landscape transformation within each pair of simulations.

When the pre-1900 natural cover was replaced with the 1993 land-use dataset, the simulated spatial patterns of the surface sensible and latent heat flux were altered significantly, resulting in changes in the structure and strength of climatologically persistent, surface-forced mesoscale circulations—particularly the afternoon sea-breeze fronts. This mechanism was associated with marked changes in the spatial distribution of convective rainfall totals over the peninsula. When averaged over the model domain, this redistribution was reflected as an overall decrease in the 2-month precipitation total. In addition, the domain average of the diurnal cycle of 2-m temperature was amplified, with a noted increase in the daytime maximum. These results were consistent among all three simulated periods, and largely unchanged when subjected to a number of model sensitivity factors. Furthermore, the model results are in reasonable agreement with an analysis of observational data that indicates decreasing regional precipitation and increasing daytime maximum temperature during the twentieth century.

These results could have important implications for water resource and land-use management issues in south Florida, including efforts to restore and preserve the natural hydroclimate of the Everglades ecosystem. This study also provides more evidence for the need to consider anthropogenic land-cover change when evaluating climate trends.

1. Introduction

Since the arrival of colonial settlers, anthropogenic activities have transformed the landscape of the Florida peninsula. Much of the transformation within south and central Florida occurred during the twentieth century, when the pace of urbanization over coastal areas and agricultural production over the interior substantially increased. During this period, natural surface hydrologic features were altered and diverted for irrigation and do-

mestic use, as well as for flood prevention, particularly in the Everglades and the Kissimmee River basin. Prior to the construction of canals and levees, much of the surface runoff of the peninsula drained into the wide, perpetually inundated floodplain of the Kissimmee River, which in turn drained southward into Lake Okechobee. Natural flow over the south rim of Lake Okechobee spilled into the wide expanse of the Everglades. The surface hydrologic budget of the Everglades was dominated by evaporation and transpiration, with surface runoff into Florida Bay composing a relatively small percentage of the annual rainfall (Kushlan 1990). Following the major water diversion projects of the early and middle twentieth century, much of the Kissimmee

Corresponding author address: Curtis H. Marshall, Dept. of Atmospheric Science, Colorado State University, Fort Collins, CO 80523.
E-mail: curtis@atmos.colostate.edu

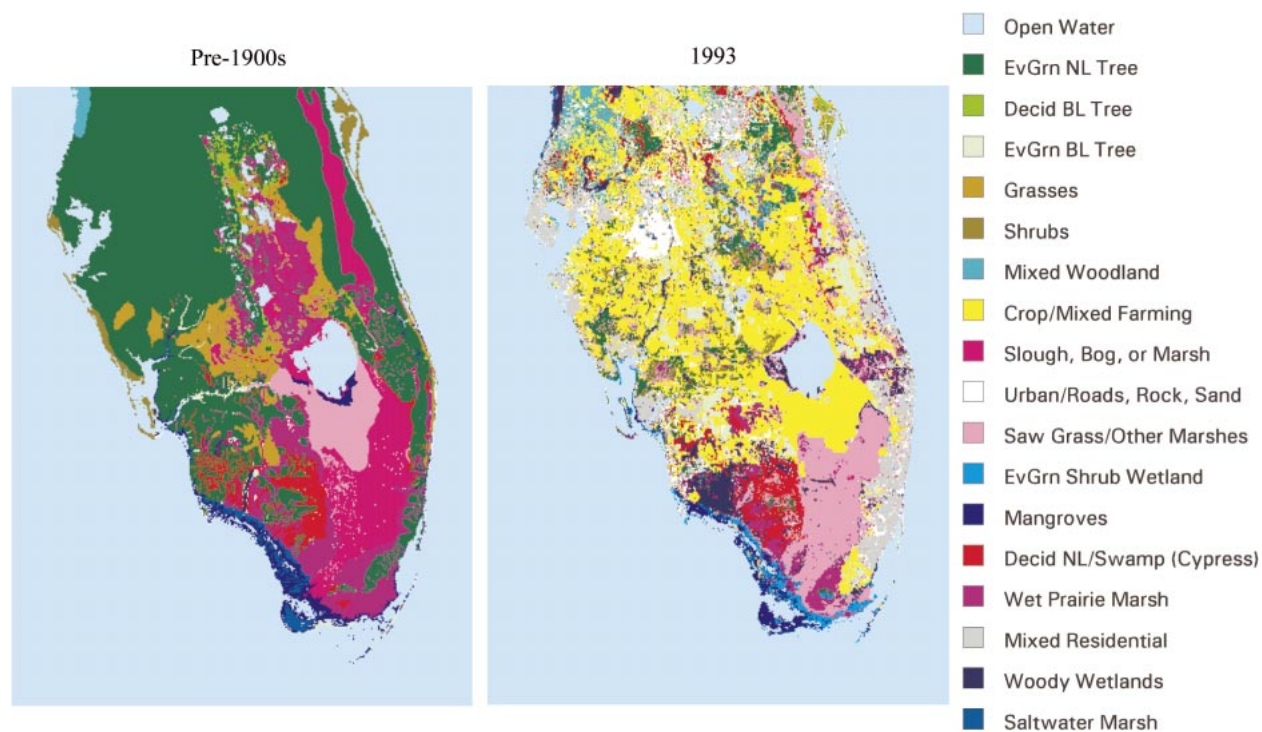


FIG. 1. USGS land-cover data for (left) pre-1900 natural land cover and (right) 1993 land use.

River basin had been drained, and the south shore of Lake Okeechobee had been dammed.

A comparison of maps that represent pre-1900 natural land cover and 1993 land-use patterns (Fig. 1) clearly demonstrates the significant changes that have occurred throughout Florida over the twentieth century. Within the Everglades, agriculture and extensive saw grass have displaced the natural saw grass plains and the freshwater marsh/slough areas. The area of freshwater marshes around and to the north of Lake Okeechobee (in the Kissimmee River basin) has been drained and converted to mixed agriculture and pasture. The current land-use patterns in the interior, central portion of the Florida peninsula, including extensive mixed agriculture, cities, roads, residential areas, and urban complexes, have collectively supplanted much of the predominantly pine forest areas of the natural landscape. The question of interest for this paper is whether these land-cover changes have affected the warm season climate of the region.

Several previous studies have addressed the impacts of land-cover change on warm season climate over spatial scales similar to the Florida peninsula, with a particular focus on surface-forced circulations and their relationship to the spatial distribution of cumulus convective rainfall (Anthes 1984; Wetzel 1990; Segal and Arritt 1992; Dalu and Pielke 1993; Pielke et al. 1999; Pielke 2001; Weaver and Avissar 2001). Over the Florida peninsula, the dominant mode of convection during the warm season is associated with the sea-breeze fronts (Byers and Rodebush 1948; Pielke 1974; Michaels et

al. 1987; Simpson 1994). Because the sea breezes are driven primarily by contrasting thermal properties between the land and adjacent ocean, it is possible that alterations in the nature of the land cover of the peninsula have had impacts on the physical characteristics of these circulations (Pielke and Cotton 1977; Gannon and Warner 1990; Baker et al. 2001). This mechanism could have important implications for the distribution of sea-breeze convective rainfall. Furthermore, it is possible that changes in land cover may have impacted other (inland) mesoscale circulation features (and related convective rainfall), as well as the diurnal cycle of surface thermodynamics (e.g., surface energy fluxes and shelter-level temperature).

In this paper, the previous study by Pielke et al. (1999) is revisited and significantly expanded upon by presenting additional simulations of the warm season weather of the Florida peninsula. These simulations were performed using the Regional Atmospheric Modeling System (RAMS; Pielke et al. 1992). In the previous study, the authors presented three simulations spanning the period July–August 1973 wherein the model configuration was identical, with the exception of the definition of land-cover. One each of the three simulations employed a land-cover database valid for 1900, 1973, or 1993. However, those simulations were limited in scope, primarily because they were performed only for a single warm season period. Furthermore, the impacts of land-cover change were not examined in the context of other model factors that are known to influ-

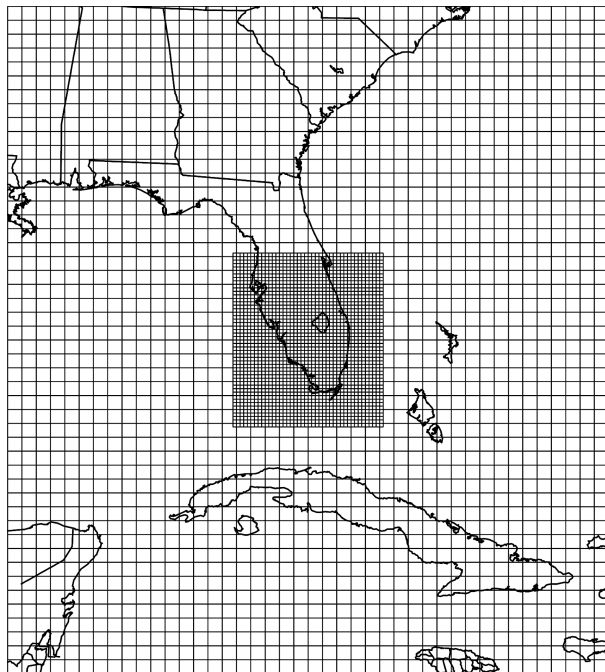


FIG. 2. Grid configurations for the RAMS domain used in this study.

ence strongly the numerical simulation of warm season convective rainfall and near-surface sensible weather. In this current work, additional simulations were performed for three separate warm season periods, and the results were subjected to a number of model sensitivity factors. Furthermore, new land-cover datasets were constructed for use in the new simulations presented in this paper. These datasets are highly detailed and considerably more realistic than those used by Pielke et al. (1999).

2. Model configuration and methodology

a. Land-use data

Land-cover datasets representing pre-1900 natural cover and 1993 land use were developed by the United States Geological Survey (USGS) in support of this study. Figure 1 shows the dominant classes for each dataset. These data, which incorporate several improvements relative to the datasets used by Pielke et al. (1999), were constructed for use in the RAMS land surface parameterization, Land Ecosystem–Atmosphere Feedback 2 (LEAF-2; Walko et al. 2000). The data domains, covering the southeastern United States at 1-km grid spacing and most of Florida at 100 m, were designed to span the RAMS model outer and inner grid domains shown in Fig. 2 (the RAMS grid configuration is described in section 2b). Use of these datasets required the number of existing LEAF-2 classes (and related biophysical parameters) to be expanded to include sloughs, saw grass marshes, wet prairies, saltwater

marshes, mangroves, and various mixed woody wetland complexes. Water depths and hydroperiods for freshwater marshes were categorized according to Kushlan (1990). The hydroperiod was defined as that time of year during which the surface is inundated with standing water. A seasonally dependent water depth was determined by the type of wetland complex. All other land-cover classes in the datasets were defined in terms of the existing LEAF-2 categories. With the addition of the classes shown in Fig. 1 to those already existing in LEAF-2, 40 categories were available for use in the simulations presented in this paper.

A Geographic Information System (GIS) was employed by the USGS to combine a variety of data sources to develop the updated land-cover datasets. Early vegetation maps, historical analyses, and paleodata studies were the primary inputs for the pre-1900 dataset. The reconstructed natural vegetation for the Everglades (south of the Kissimmee River watershed) was derived mainly from a GIS analysis of the Davis (1943) South Florida Natural Vegetation Map, as adapted by McVoy (1996), McVoy et al. (2003), and Willard et al. (2001). McVoy (1996) analyzed historical documents and early photographs to reconstruct the distribution of saw grass and slough/bogs/marshes in the Everglades prior to conversion to agriculture and the diversion of surface water flow by the construction of surface hydrology controls [a historical review of water resource engineering activities is provided by Light and Dineen (1994)]. Subsequently, Willard et al. (2001) presented evidence based on paleostudies of pollen data extracted from core samples within the Everglades to support the analysis of McVoy. Given these historical and paleovegetation studies, the pre-1900 land-cover dataset is believed to closely approximate the vegetation patterns that existed in the Everglades prior to large-scale human disturbance activities. The predisturbance land-cover data constructed by Costanza (1975, 1979) was used for the Kissimmee River watershed. The Küchler (1964) potential natural vegetation dataset was used as the primary source of pre-1900 data for the remainder of Florida and the southeastern United States, with two modifications. First, the southern mixed forest class was modified to a predominantly evergreen needle leaf forest, which represents the extensive areas of longleaf pine and Florida slash pine in fire-prone areas (Landers and Boyer 1999). Second, the data were modified to account for the freshwater marsh areas of the southern St. Johns River basin (note the axis of marsh over the east-central peninsula shown in Fig. 1, just inland of Cape Kennedy, southward to the latitude of the north shore of Lake Okeechobee).

The 1993 land-cover datasets were derived from the USGS 30-m National Land Cover Data dataset (NLCD; Vogelmann et al. 1998, 2001) and the 30-m Florida Gap Analysis Project (GAP) dataset (Pearlstone et al. 2002). The USGS NLCD, which was developed for the conterminous United States based on 1992–93 Landsat Thematic Mapper (TM) data, was used for the RAMS outer

grid within the southeastern United States. The 1993 land-cover data for the model inner grid was derived by combining the NLCD for Florida with the GAP data. The GAP land-cover product was developed by the USGS (Biological Resources Discipline), the Florida State Cooperative Fish and Wildlife Research Unit, and the University of Florida using Landsat TM scenes from the 1992–94 time frame. Urban, residential, mixed agriculture, and other standard classes were selected from the NLCD, while wetlands, forests, and dry prairies were selected from the GAP data.

b. RAMS model configuration

RAMS version 4.3 was used for the numerical simulations presented in this study. All of the simulations were performed on a nested grid configuration (Fig. 2), with an outer grid of 42×48 points at a 40-km interval, covering the southeast Atlantic and Gulf Coast states, southward to the latitude of the Yucatán Peninsula. An inner grid with 42×50 points at 10-km spacing was nested to cover central and south Florida and adjacent coastal waters. Both grids extended over 30 vertical levels, with the lowest level near 100 m above ground level. The vertical grid spacing was geometrically increased with height to a maximum of 1 km at the model top (20 km). A 1-min time step was employed on the outer grid, with 30 s on the inner grid. Forward–backward first-order time differencing was used with a split-explicit scheme for filtering fast modes (Tripoli and Cotton 1982). Initial conditions and outer grid lateral boundary conditions were provided by the National Centers for Environmental Prediction–National Center for Atmospheric Research (NCEP–NCAR) global reanalysis dataset (Kalnay et al. 1996). During the integration of the simulations, the reanalysis data were updated every 6 h and nudged over the five outer grid points at each time step. Note that the simulation time period (e.g., July–August 1973) was determined by using the reanalysis data valid for that period. The Kain–Fritsch (1993) scheme was used for representing the effects of unresolved, precipitating deep convection on the model grid scale. The radiative transfer scheme of Mahrer–Pielke (1977) was used to parameterize the vertical flux of short- and longwave radiation. Anisotropic deformation (Smagorinsky 1963) was employed to represent subgrid-scale turbulent fluxes, along with the Louis (1979) representation of the surface exchange coefficients.

The surface energy budget was represented by LEAF-2, which partitions the net radiation into sensible, latent (evaporation plus transpiration), and soil heat fluxes. This scheme contains prognostic equations for soil moisture and temperature. The subgrid “tile approach” (Walko et al. 2000) was used to allot each RAMS model grid cell four separate land-cover classes (including water). These four classes were chosen by their frequency of occurrence within a RAMS grid cell, as determined

from aggregation of the original pre-1900 and 1993 datasets that are described above. The soil model consisted of 11 vertical layers spanning a depth of 2 m. The initial soil temperature was determined by an offset of the initial air temperature in the first atmospheric layer above ground. Initial soil moisture for the top layer was set to 40% of the saturation value. This percentage was increased with depth to a maximum of 60% at 50 cm and below. The soil moisture saturation value for a LEAF-2 tile was defined by using a spatial distribution of soil types, which was adapted from the global 3-km database provided by the Food and Agriculture Organization (FAO) of the United Nations (FAO 1997). Soil moisture was initialized at complete saturation if the overlying vegetation class was identified as a swamp or marsh type. These classes, covering much of the Everglades region in both land-cover cases and the Kissimmee River valley in the pre-1900 dataset, were inundated with 10 cm of standing water. It will be shown that the presence of standing water had important impacts on the simulated surface energy budget of those regions. The SST was specified using the 1° monthly climatological dataset available from NCEP (Reynolds and Smith 1994).

c. Experimental design

Pairs of simulations were completed for July–August of 1973, 1989, and 1994. Within a given pair, one member employed the pre-1900 land cover, while the other used the dataset valid for 1993. The 1989 and 1994 warm season periods were chosen for simulation because they correspond, respectively, to drought and above-average conditions with respect to precipitation climatology over the peninsula. These two periods are also very close to the valid time for the 1993 land-use data. Thus, choice of these periods permits us to address the question of how simulation results for relatively wet and dry periods would be changed if current land cover were replaced with natural cover. Before undertaking these simulations, the simulations for the period July–August 1973 that were presented in the previous work of Pielke et al. (1999) were repeated. Even though this current work does not include any simulations that employ the 1973 land-cover dataset used in that study, it was thought useful to repeat those simulations in order to ascertain the impact of the improvements in the pre-1900 and 1993 land-cover datasets. In addition to improved land cover, the RAMS model configuration used in this present work included the Kain–Fritsch convective parameterization scheme. The simulations presented by Pielke et al. (1999) used the Kuo (1974) scheme. It will be shown that the choice of convective parameterization had a substantial impact on the results.

Because of the public attention given to the perceived increase in the frequency and severity of drought in south Florida during the last century (e.g., Boyle and Mechem 1982), the 1989 “dry” set of simulations was

chosen for additional analysis. Specifically, these simulations were used to investigate the impact of changing the land cover on the near-surface wind field and the diurnal cycle of shelter-level temperature. It will be shown that the change in land cover had significant impacts on the numerically simulated, three-dimensional structure of the sea-breeze circulations and hence on the dominant mode of convective precipitation over the domain. The 1989 period was also chosen for subjecting the results to a number of model sensitivity factors. Specifically, simulations were conducted wherein the model configuration was altered to investigate the sensitivity of the results to horizontal grid spacing and to the choices for the convective and radiation parameterizations. In addition, the sensitivity of the results to initial soil moisture and the specification of SST on the regional model grid was examined. The details of the design of these experiments and the requisite changes to the model configuration are described in section 4.

3. Results

a. Precipitation

Comparison of the observed precipitation for the three simulated periods (Fig. 3) illustrates that the 1973 and 1994 periods were relatively wet, whereas the 1989 period was relatively dry, as discussed above. During the 1973 period, totals exceeded 450 mm over many areas of the western and southern peninsula. Totals for 1994 exceeded this threshold at several locations, with a few areas above 550 mm. Areas receiving more than 450 mm during the 1989 period are confined to the southwestern portion of the peninsula, with appreciably less over northern and central portions in comparison to 1994 and 1973. The July–August accumulated precipitation fields from the RAMS simulations (Figs. 4–6) illustrate that the model was able to capture the observed magnitudes with a reasonable degree of success. The overall magnitudes (with either land-cover scenario) are also relatively dry for the 1989 period, in accordance with the relative magnitudes in the observational fields. For all three periods, larger totals were realized with the use of the pre-1900 land cover. The difference fields (bottom panels of Figs. 4–6; 1993 minus pre-1900 scenario) show decreases over much of the domain when the 1993 land use was employed. South of the latitude of Tampa Bay, decreases are noted along parallel axes that run roughly north to south, between the coasts and the Kissimmee River basin. Interestingly, when the precipitation fields are averaged in space over all land grid points in the domain, all three

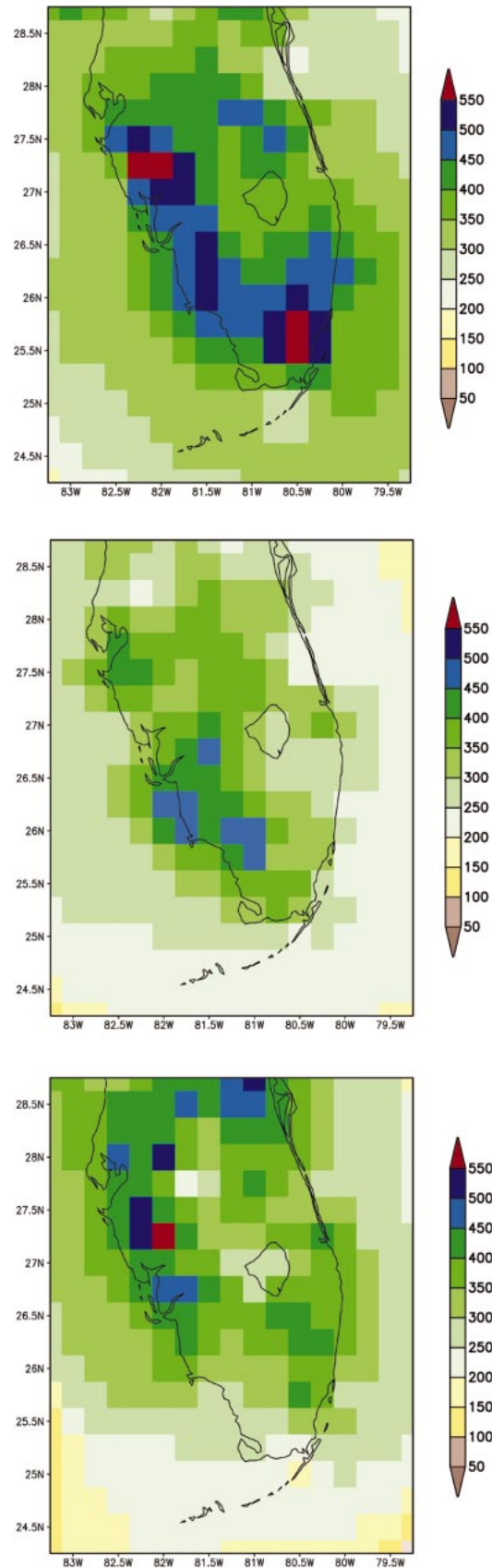


FIG. 3. Accumulated precipitation (mm) from the CPC analysis of cooperative observation network rain gauge data (analysis on 0.25° grid) for (top) Jul–Aug 1973, (middle) Jul–Aug 1989, and (bottom) Jul–Aug 1994.

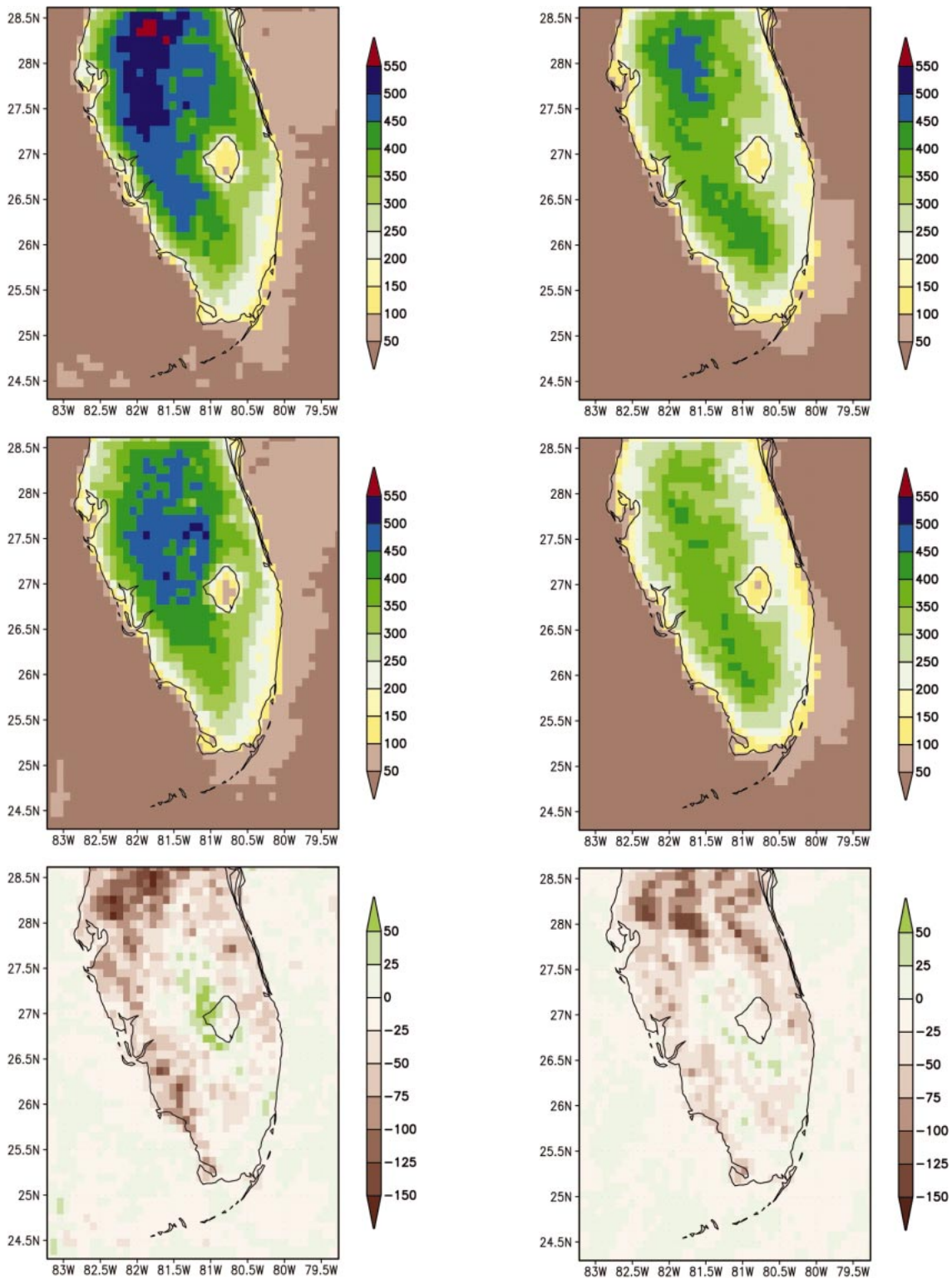


FIG. 4. Accumulated convective rainfall (mm) from the model simulations of Jul–Aug 1973 with (top) pre-1900 land cover, (middle) 1993 land use, and (bottom) the difference field for the two (1993 minus pre-1900 case).

FIG. 5. Same as Fig. 4, except for Jul–Aug 1989.

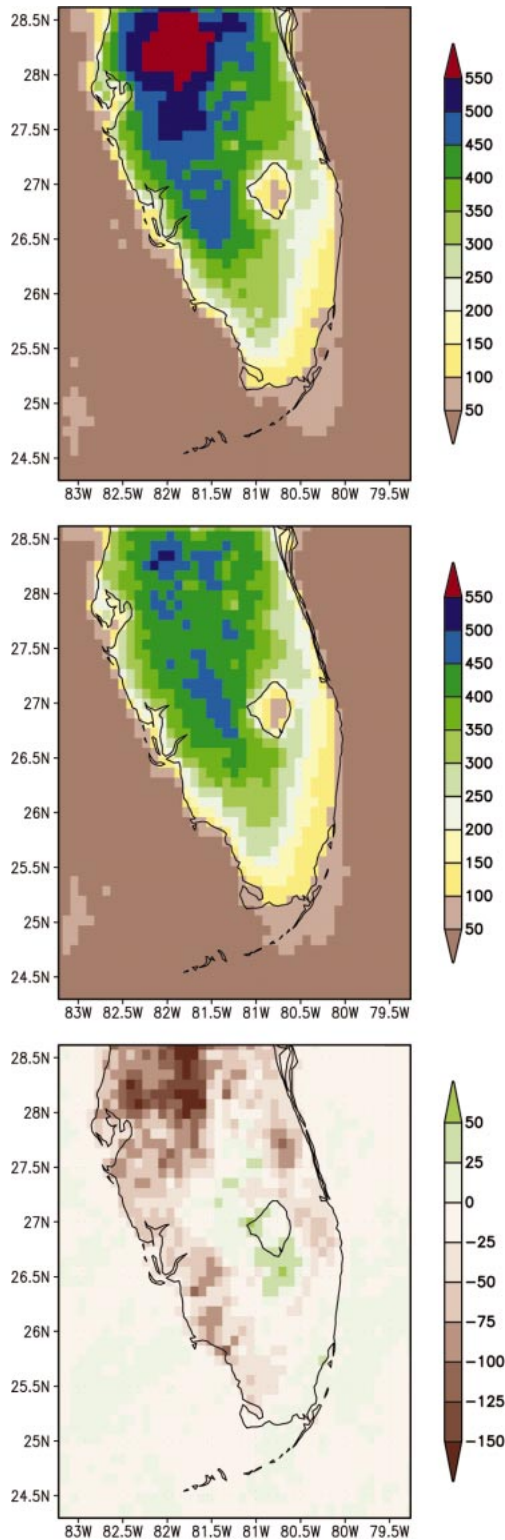


FIG. 6. Same as Fig. 4, except for Jul–Aug 1994.

of the resulting difference field values correspond to a 10%–12% decrease of their respective pre-1900 value.

Despite the consistent decrease in the grid-average value, precipitation increased along a north–south axis in the interior peninsula in all the three simulated periods when the 1993 land-use dataset was employed. Comparison with Fig. 1 shows that the area where these rainfall increases are found corresponds spatially to an axis of wetlands that was drained and converted to agriculture during the twentieth century. Note that the parallel axes of decrease discussed above that are juxtaposed to either side of this central axis of increase are consistent with the position of the afternoon sea-breeze fronts (Michaels et al. 1987). More evidence will be presented in later sections to suggest that these patterns are associated with marked changes in the climatological characteristics of mesoscale circulations that are associated with the land cover in this region.

In comparing these results and those presented in the study by Pielke et al. (1999) with the observational data, it is apparent that the new model configuration, with updated land-cover datasets and the Kain–Fritsch convective scheme, provided improved rainfall totals for the 1973 period. The model results shown in Pielke et al. (1999) illustrate that the old configuration yielded July–August 1973 rainfall totals that were under 300 mm for the 1993 land-cover case, with totals less than 320 mm for the pre-1900 scenario. The newer magnitudes are generally larger and closer to the observed. As noted above, the new model results also capture the general magnitudes for the 1989 and 1994 periods. However, there are some differences in the spatial details between the observations and the new model results. It should not be expected that the model would exactly resolve the finescale details of the accumulated field over the course of a 2-month integration. It is also worth noting that the observational dataset shown here may not perfectly represent the spatial distribution of the rainfall that actually fell. For example, the greater values in the observations over the open ocean could be an artifact of the nature of the Cressman analysis scheme (Cressman 1959) that is used by the Climate Prediction Center (CPC) to produce these objectively analyzed rainfall fields. The model results indicate that relatively little precipitation fell over the open ocean. The Cressman scheme extrapolates the rain gauge point values over land to the nearby ocean, because no gauge observations are available over the ocean to influence the analysis value. Despite discrepancies of this nature with the model results, and some disagreement between the model and observed spatial distributions, the simulations appear to provide a reasonable distribution of rainfall totals.

b. Surface fluxes

The patterns of average sensible and latent heat flux for the July–August 1973 simulations (Figs. 7 and 8)

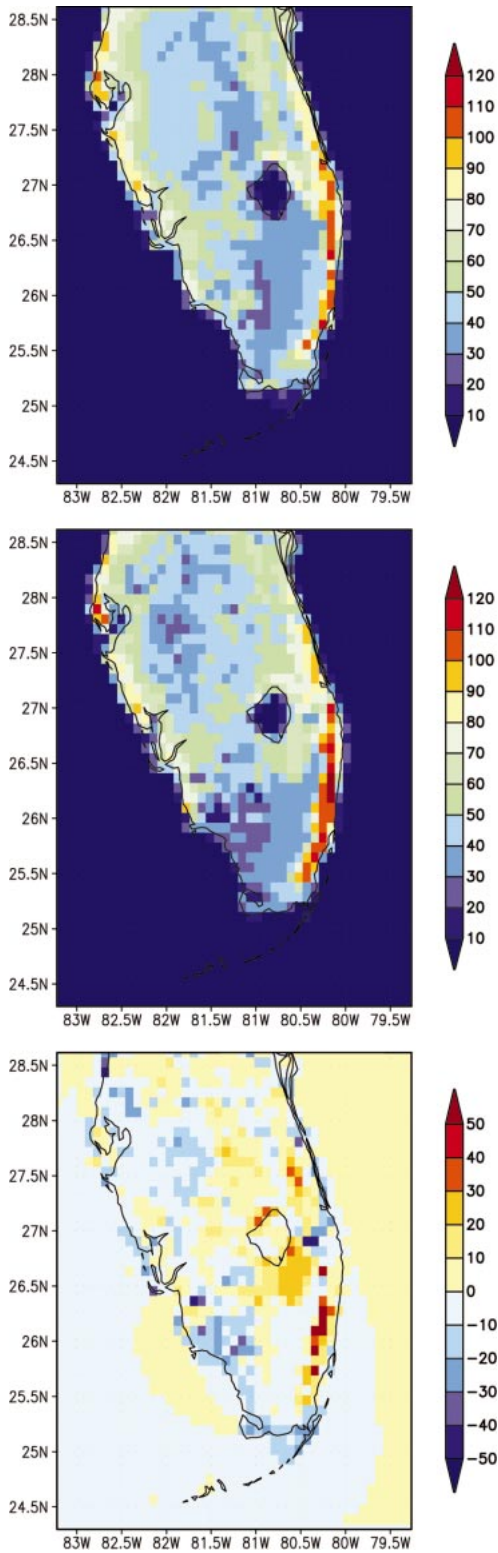


FIG. 7. Two-month average of the surface sensible heat flux ($W m^{-2}$) from the model simulations of Jul–Aug 1973 with (top) pre-1900 land cover, (middle) 1993 land use, and (bottom) the difference field for the two (1993 minus pre-1900 case).

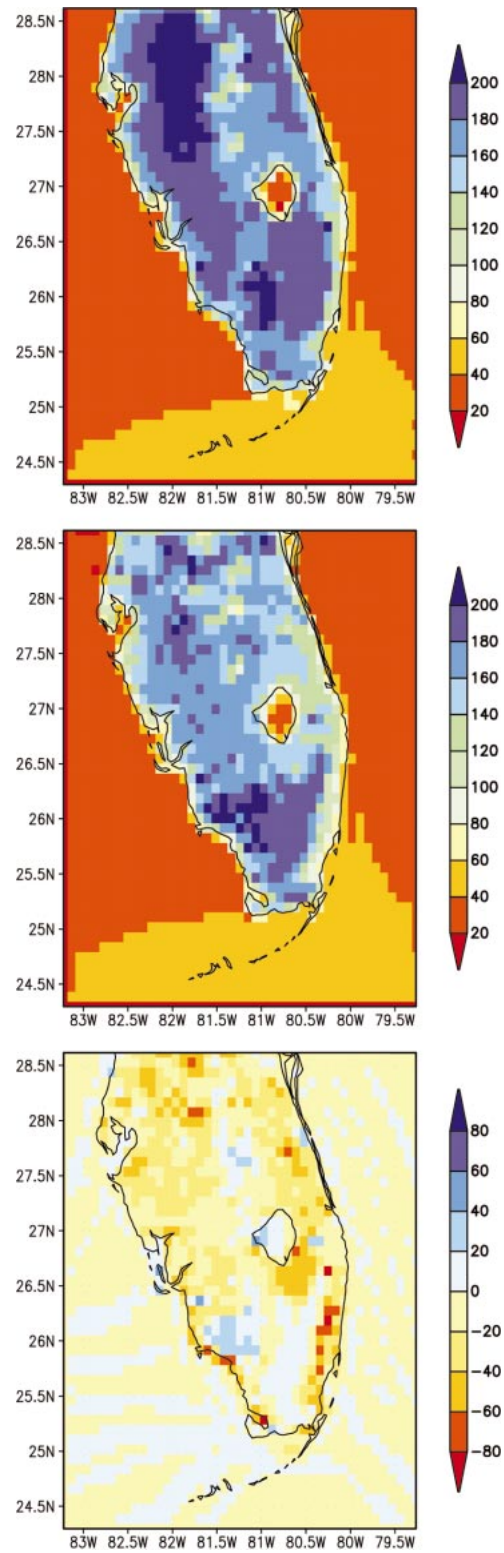


FIG. 8. Two-month average of the surface latent heat flux ($W m^{-2}$) from the model simulations of Jul–Aug 1973 with (top) pre-1900 land cover, (middle) 1993 land use, and (bottom) the difference field for the two (1993 minus pre-1900 case).

are in general physical agreement with the previous results in Pielke et al. (1999). Of particular interest is the distinct axis of increased sensible heat flux in the difference field that extends along the Kissimmee River basin to south of Lake Okeechobee. This increase is associated with the draining of the Kissimmee floodplain (Fig. 1) and the draining and conversion to agriculture of the area south of Lake Okeechobee. Another distinct axis of increase is noted along the eastern coastal ridge, which appears to be associated with urbanization. Figures 9–12 show the same general patterns in sensible and latent heat flux for the 1989 and 1994 periods. Interestingly, and similar to the model precipitation results, the grid average of the latent heat flux difference fields exhibits a consistent decrease of near 10% of the grid-average pre-1900 value. However, the grid-average sensible heat flux is nearly unchanged, despite the coherent patterns of increase over the central portion of the peninsula. The grid average, in this case, reflects the considerable subgrid-scale spatial variability in the difference field.

The spatial characteristics of the sensible and latent heat flux and precipitation fields for the 1989 simulations, and their associated changes between the two different land-cover scenarios, appear to be the most physically and visually distinct when compared to the physical changes in land cover shown in Fig. 1. In addition, the 1989 period was during and following a considerable drought over the south Florida region (Schmidt et al. 2001). Because of these factors, and because the popular interest in possible increases in drought during the twentieth century has provided part of the motivation for this study, the 1989 simulations were chosen for further analysis. Specifically, detailed analysis of the diurnal cycle of shelter-level temperature, the characteristics of the low-level wind patterns, and various sensitivity studies were undertaken.

c. Diurnal cycle of shelter-level temperature

Figures 13 and 14 show the 2-month average of the simulated 2-m daily maximum and minimum temperatures. While there is a great deal of spatial variability in these fields, the results show that daytime maximum generally increased with the use of the 1993 land cover. Significant decreases in daily minimum were realized along the interior axis of the peninsula. When averaged for all land grid points in the domain, the complete diurnal cycle of shelter-level temperature is amplified (Fig. 15a). The amplification is particularly apparent at locations where standing water has been drained, such as the grid point in the heart of the Kissimmee River basin marked by the “X” in Figs. 13 and 14 (Fig. 15b). At this particular point, the nighttime minimum is nearly 4°C cooler in the 1993 scenario, and the daytime maximum is warmer and phase-shifted considerably earlier in time. The phase-shifted and decreased maximum is consistent with the fact that the standing water present

at this location in the pre-1900 case should result in a higher effective thermal inertia of the land surface relative to the 1993 case. For a typical diurnal cycle in the pre-1900 case, more net radiation should be expended after sunrise to heat the standing water, thus delaying the commencement of sensible heating of the lower atmosphere. The decrease in nighttime minimum is also consistent with a reduced heat capacity of the land surface, because this could permit more efficient radiational cooling.

d. Mesoscale circulations

During midsummer, light easterly flow is typically present over the central and southern Florida peninsula, in association with the western extension of the dominant high pressure system over the subtropical Atlantic Ocean. The flow pattern is characterized by general synoptic quiescence. Under this regime, the sea breezes are often the most meteorologically significant circulation features, and on many afternoons, convection occurs in association with them. During the typical diurnal cycle, breezes form on both the east and west coasts of the peninsula and penetrate inland with the intensification of afternoon heating. The west coast front typically does not penetrate as far inland as the east coast one because of interaction with the large-scale easterly flow. However, this interaction usually results in stronger convergence and greater precipitation along the west coast breeze. According to an analysis of radar data by Michaels et al. (1987), convection begins first over the western side of the peninsula, and that is typically where the greatest warm season rainfall occurs. This maximum is apparent in the observations shown in Fig. 3, as well as in the model results shown in Figs. 4–6. Pielke (1974) provides observational and modeling evidence that outlines these patterns and this sequence of events as the typical diurnal evolution of the sea breezes over the Florida peninsula.

The fundamental mechanism behind the formation and maintenance of the sea breezes is the gradient of surface sensible heat flux between land and sea. Thus, it stands to reason that changes in the nature of the underlying land surface, which serve to alter the spatial patterns of sensible heat flux, could have a direct impact on the structure and diurnal evolution of the sea breezes. The spatial distribution of land surface properties could also be associated with other (inland) mesoscale flow features that could be significant in terms of convection in their own right or in their ability to interact with the sea breezes. Figure 16 shows the 2-month average of the near-surface (10 m) wind field at 1600 UTC for the July–August 1989 pair of simulations, with the derived surface divergence field. The time of day chosen for analysis (1600 UTC) corresponds closely to local solar noon, and the pattern shown is typical for the near-surface wind field just before convection initiates (Michaels et al. 1987). Thus, the effects of the land surface

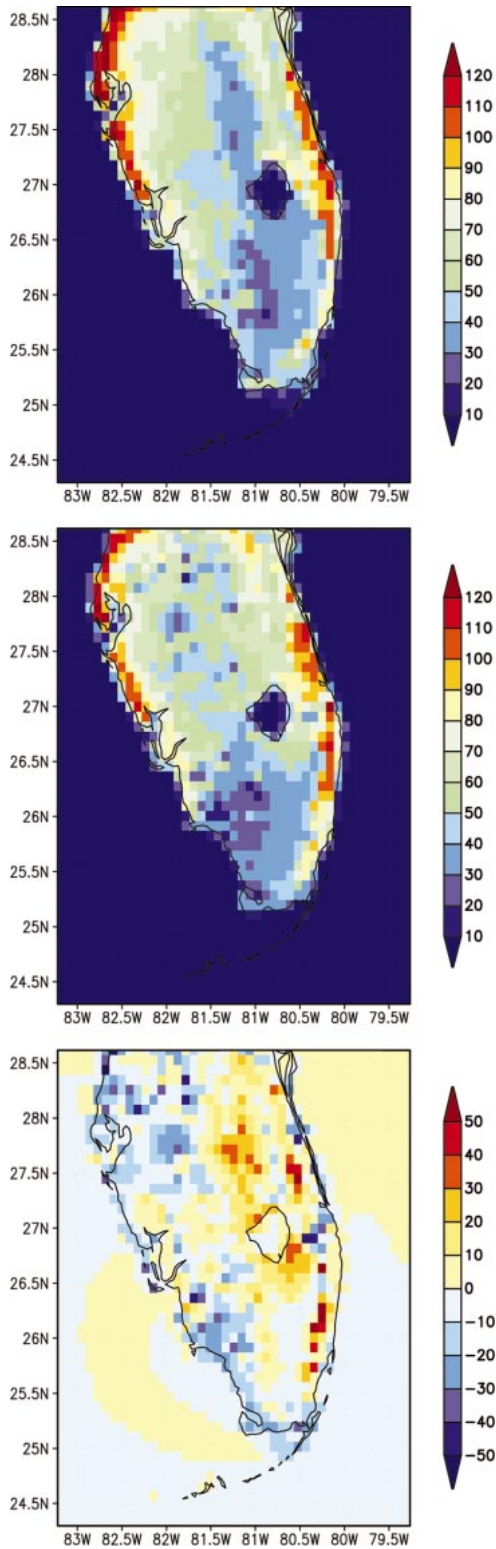


FIG. 9. Same as Fig. 7, except for Jul-Aug 1989.

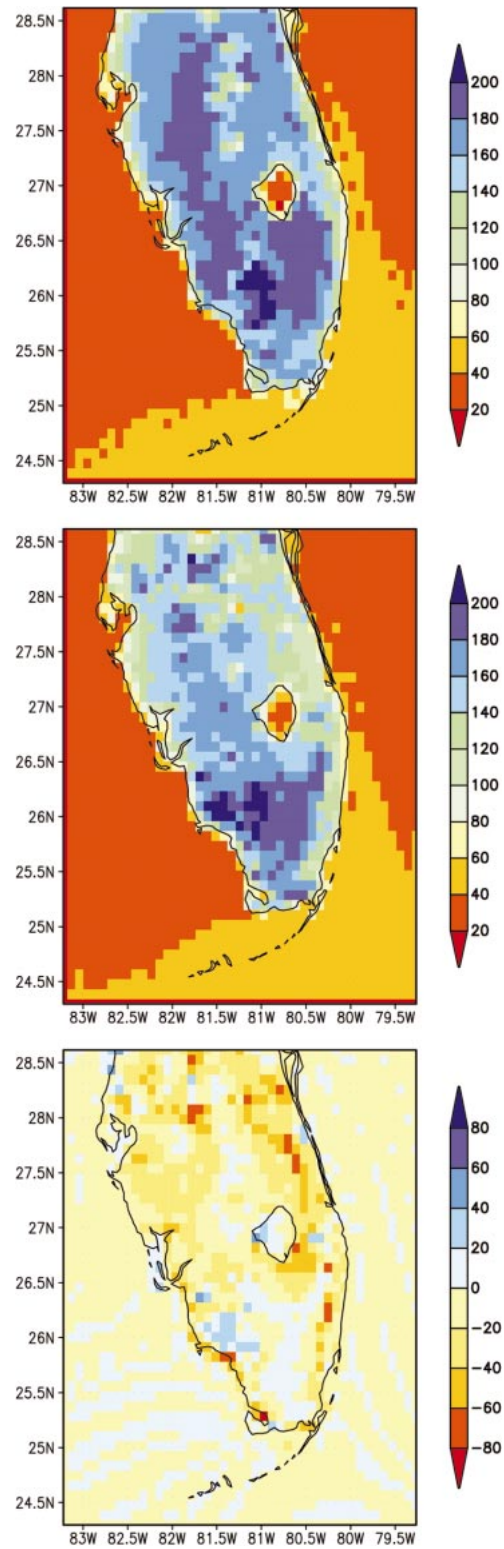


FIG. 10. Same as Fig. 8, except for Jul-Aug 1989.

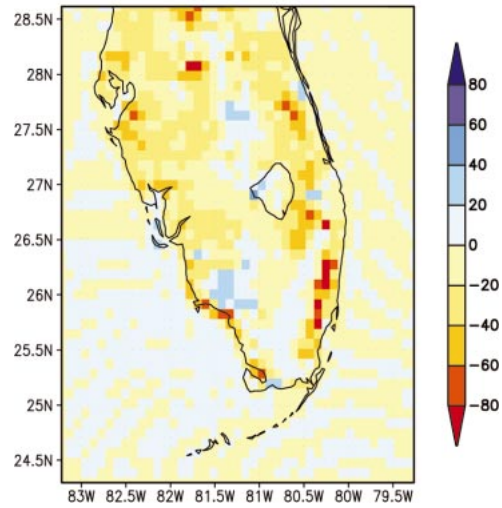
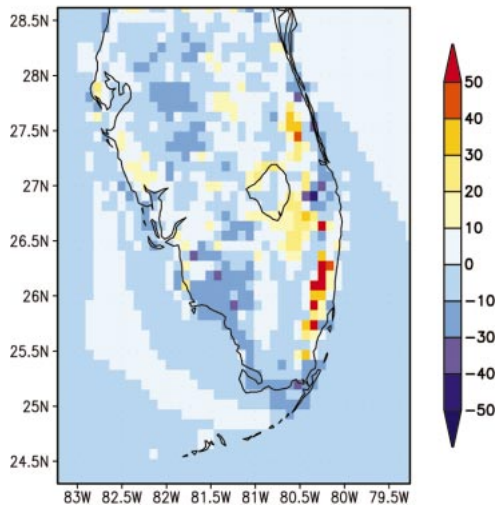
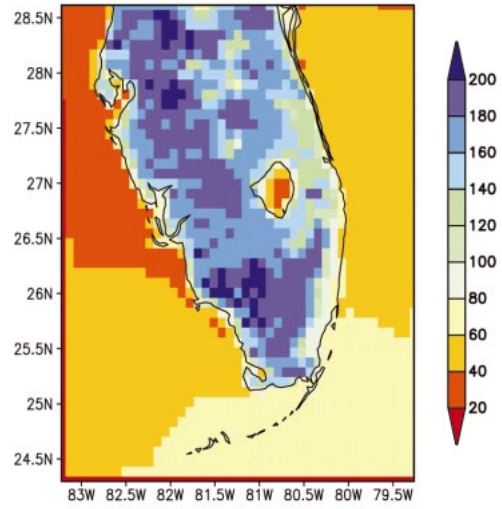
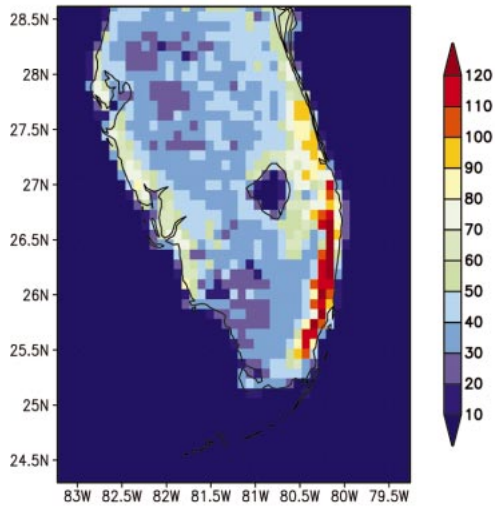
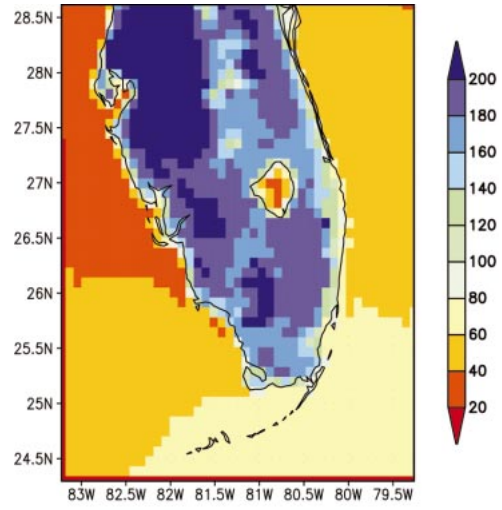
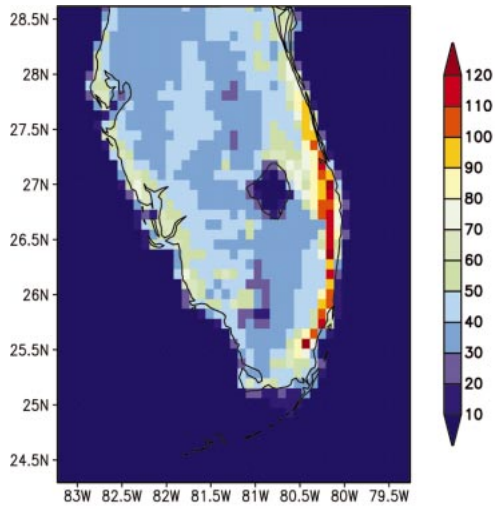


FIG. 11. Same as Fig. 7, except for Jul–Aug 1994.

FIG. 12. Same as Fig. 8, except for Jul–Aug 1994.

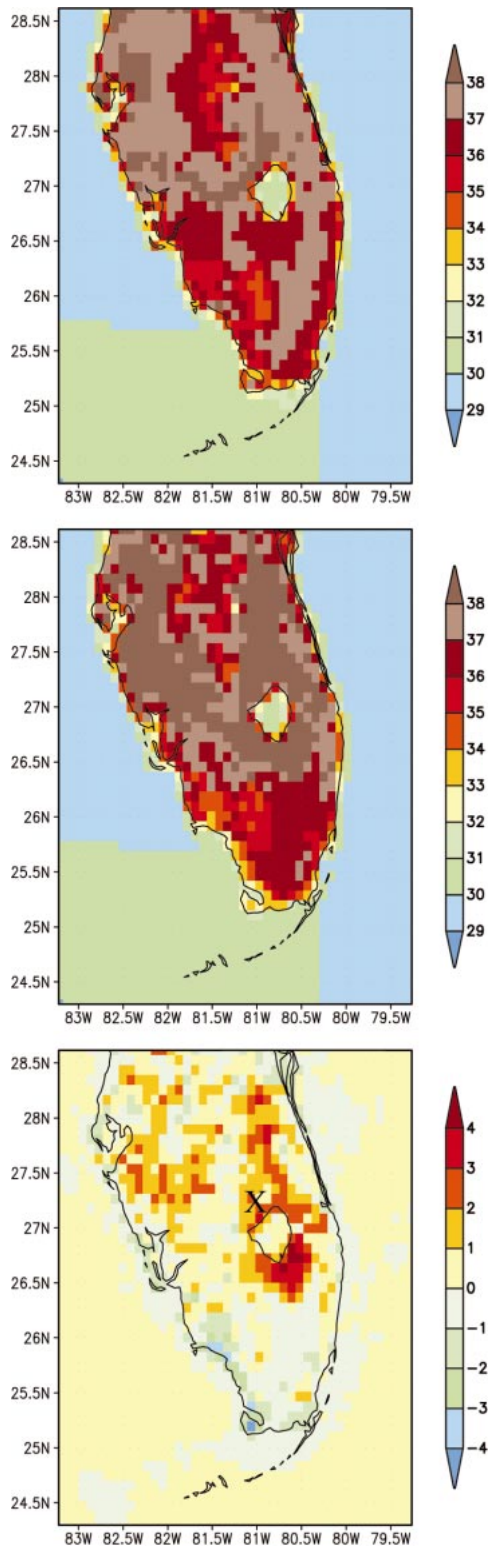


FIG. 13. Two-month average of the daily max shelter-level temperature from the model simulations of Jul–Aug 1989 with (top) pre-1900 land cover, (middle) 1993 land use, and (bottom) the difference field for the two (1993 minus pre-1900 case).

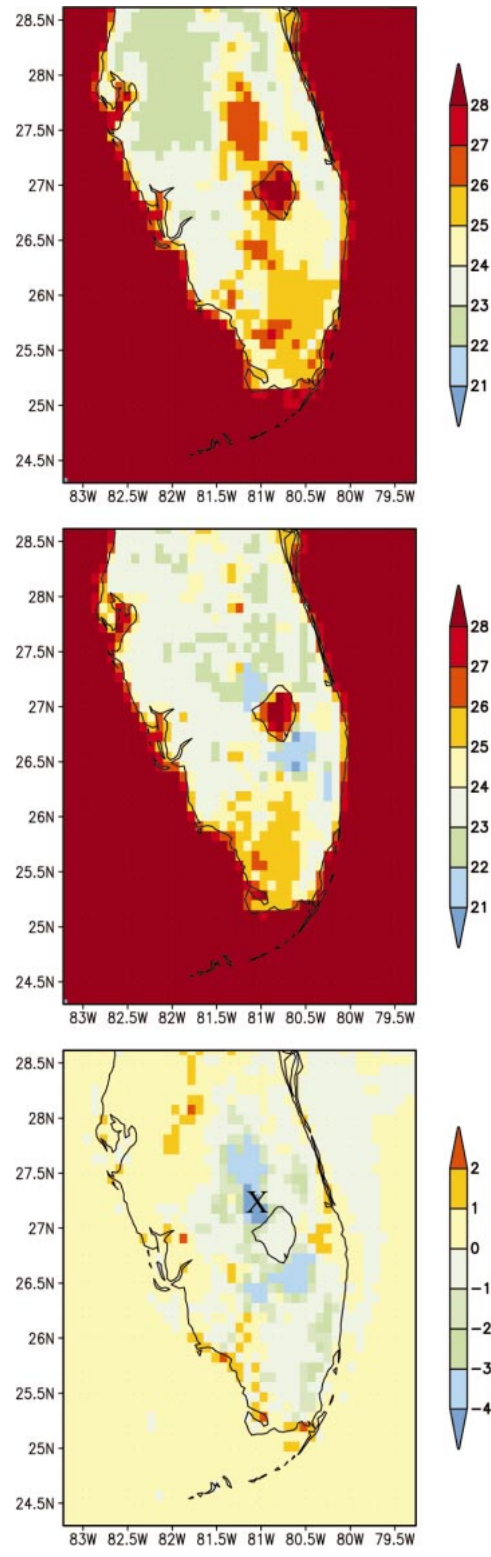


FIG. 14. Same as Fig. 13, except for daily min temperature.

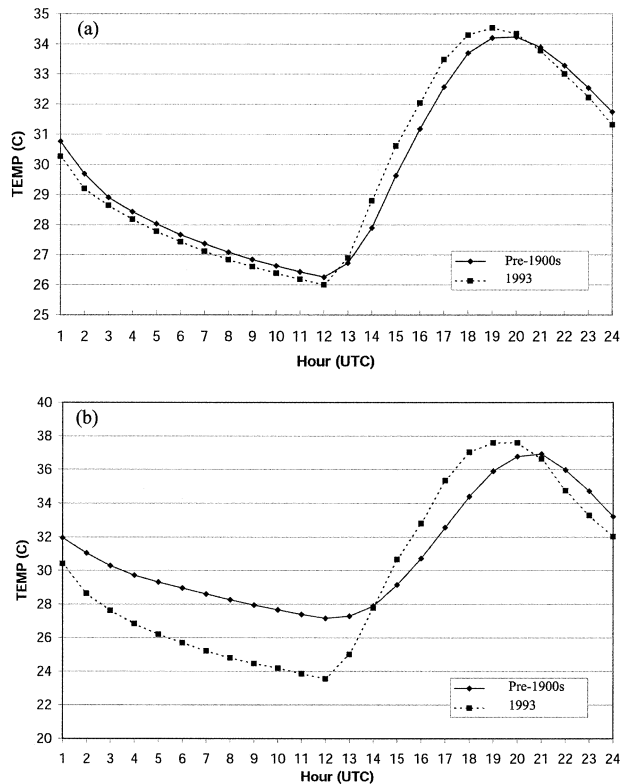


FIG. 15. Two-month average of the diurnal cycle of shelter-level temperature from the model simulations for Jul–Aug 1989 (a) averaged over all land grid points in the domain and (b) for a grid point in the Kissimmee River valley that is indicated by the “X” in Figs. 13 and 14.

are readily observable without complicating factors due to alteration of the near-surface wind by convective updrafts and downdrafts. Note the divergence–convergence couplet associated with acceleration toward the more intensely heated land along the coastlines. Note as well, particularly in the pre-1900 case, the spatially coherent axis of surface divergence (positive values) along the inundated floodplain of the Kissimmee River.

The difference of the divergence fields between the two cases (Fig. 17, color shaded field; 1993 minus pre-1900) indicates decreased values over the Kissimmee River valley. This signature is also indicated by convergence of the vectors in the horizontal wind vector difference field that is overlain on the shaded divergence field. Negative values in the divergence difference field (and accompanying convergence of the wind field difference vectors) can result from three different possibilities. The first possibility is that a grid point with convergent flow in both land-cover cases was more convergent in the 1993 case (i.e., negative values became more negative). Second, a grid point that was divergent (positive) in the pre-1900 case was convergent (negative) with the use of the 1993 land cover. The final possibility is that a point was divergent in the pre-1900 case but was *less* divergent (though not convergent) in

the 1993 case. Thus, the coherent axis of divergence along the Kissimmee basin indicated in the pre-1900 case (Fig. 16, left) that is characterized by negative values and converging vectors in the difference field (Fig. 17) represents the fact that, when the pre-1900 land cover is replaced with the 1993 data, the flow over this area becomes either less divergent or has become convergent. Close inspection shows that over a number of grid cells in the vicinity of the Kissimmee River, divergent flow in the pre-1900 case became convergent in the 1993 case. This feature appears to be spatially consistent with several features presented above. Most notably, the distinct axis of increase in the model rainfall fields (Figs. 4–6) is collocated. In addition, it is spatially aligned with the distinct axis of the increase in sensible heat flux seen in Figs. 7, 9, and 11 and the axis of increased (decreased) maximum (minimum) temperature shown in Fig. 13 (Fig. 14). These results suggest that the changes seen in these fields are related through a physical–dynamical framework that is directly attributable to the difference in the land-cover class between the two simulations.

In order to further investigate the possibility of a physical–dynamical link between changes in precipitation and changes in mesoscale flow patterns, vertical cross sections of the low-level wind flow in the x – z plane have been constructed to complement Figs. 16 and 17. Vertical cross sections of the 2-month average of the 1600 UTC u and w wind components were taken over the lowest 3000 m of the model domain (Fig. 18). The data shown in Fig. 18 are the average of all such x – z planes over the latitude belt from 26.5° to 28° N. The purpose of averaging in the north–south direction was to capture the general flow pattern associated with the distinct axis of increased precipitation along the Kissimmee River valley and the juxtaposed axes of decrease. The concentrated areas of upward vertical velocity associated with the sea breezes are shown along the flanks of the domain in both land-cover cases, along with a broad area of subsidence in the interior. The difference field (Fig. 19; 1993 minus pre-1900) indicates a general weakening of the vertical circulations. Note the marked decrease in the upward vertical velocities along the upward branches of the sea-breeze circulations when the 1993 land-cover scenario is employed. Because these were areas of upward motion in both land-cover scenarios and the magnitude of that motion was greater in the pre-1900 case, the decrease of upward motion is indicated as downward motion in the difference field (note the regions centered around 82.2° and 80.4° W in Fig. 19). Over the central part of the domain, the general subsidence was decreased with the use of the 1993 land cover. This decrease in downward motion is shown as relative upward motion in Fig. 19 (between approximately 80.9° and 81.7° W) because the absolute magnitude of the subsidence is greater for the pre-1900 case. It is suggested that the area of generalized subsidence in the pre-1900 case is associated with the out-

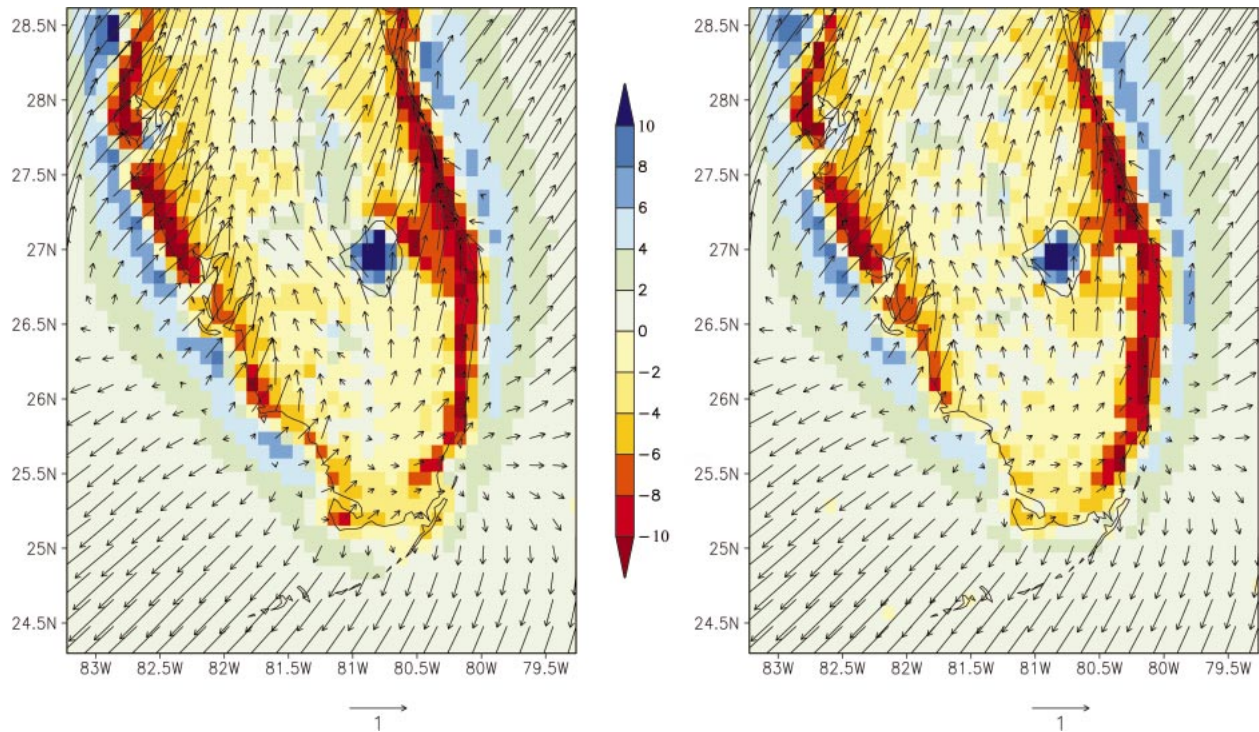


FIG. 16. Two-month average of the 1600 UTC 10-m horizontal wind (vectors) and derived divergence field (color shaded; 10^5 s^{-1}) from the simulations of Jul–Aug 1989 with (left) pre-1900 land cover and (right) 1993 land use.

ward-directed (divergent) horizontal flow over the Kissimmee River basin seen in the left panel of Fig. 16. Recall that the coherent axis of horizontal divergence over this area is greatly reduced or even replaced with weak convergence in the 1993 case. Mass continuity arguments would suggest that a decrease in compensating subsidence could occur over that part of the domain where surface divergence is weakened.

The characteristics of the changes in the low-level horizontal wind field patterns and associated vertical circulations may be associated with the changes in sensible heat flux patterns shown in Figs. 7, 9, and 11. In the framework of the pre-1900 land-cover scenario, the expanse of the Kissimmee River basin may have resulted in a divergent, outward-directed mesoscale flow, because sensible heating increased outward from the center of the water-covered basin. This proposed mechanism is physically the same as that which drives the sea-breeze circulations, except that in this particular case, the sensible heating gradient arises not because of the proximity of land and sea, but because of spatial gradients in the thermal properties of the land surface. With the use of the 1993 land-cover data, wherein the inundated floodplain of the Kissimmee River basin has been drained, thereby increasing the sensible heat flux over this area, the suggested mechanism would be diminished or even removed. The effect on the mesoscale flow patterns is visually apparent in both the difference

field for the horizontal flow (Fig. 17) and the difference field of the vertical cross sections (Fig. 19).

If the outward-directed mesoscale breeze associated with this mechanism is considered in the context of the sea breezes, it stands to reason that it could serve to enhance the convergence and upward motion associated with them. This enhancement could occur because the afternoon sea-breeze fronts are often positioned immediately on either side of the Kissimmee River valley, and their associated near-surface flow is directed inward, toward the central part of the peninsula. Constructive reinforcement through this process should be most apparent in the pre-1900 land-cover case, when the outward divergence associated with the Kissimmee River basin was present. Such reinforcement would be either decreased or eliminated with use of the 1993 land cover, resulting in decreased convergence along the adjacent sea-breeze fronts.

Given that preferred areas of mesoscale vertical motions could be realized in mesoscale variation of the convective rainfall, it is not surprising that those areas along the sea-breeze fronts that are marked by decreased upward motion are consistent with the axes of decreased precipitation shown in Figs. 4–6, whereas the decreased subsidence over the interior is associated with increased precipitation. This spatial pattern of the changes in the accumulated rainfall between land-cover scenarios, readily apparent in a visual inspection of the model

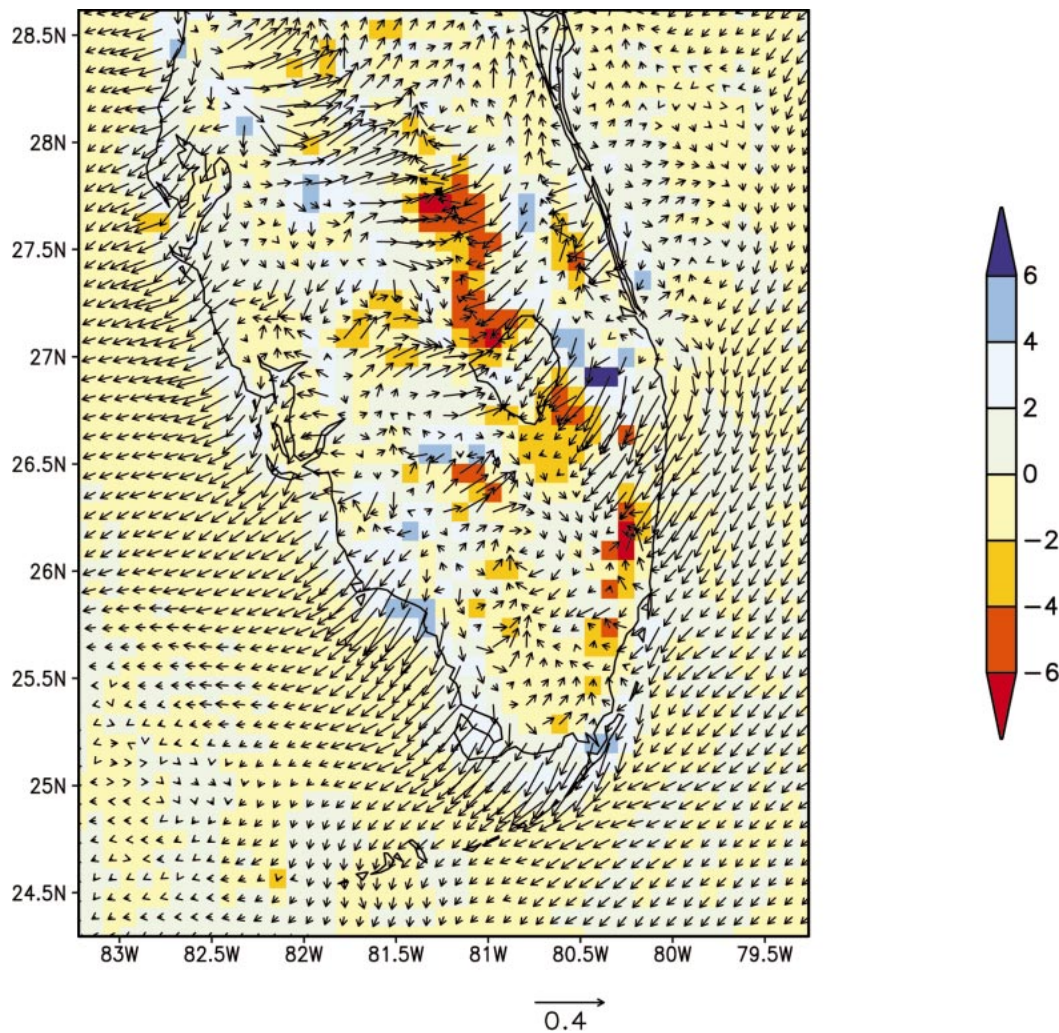


FIG. 17. Difference (1993 minus pre-1900 case) of the fields shown in Fig. 16.

fields, is consistent among all the simulated periods. The resulting grid-average rainfall decrease is also rather consistent among the three periods. As discussed above, the spatial redistribution of convective precipitation results in an overall grid-average decrease of 10% to 12% for all simulated periods. Therefore, it is suggested that the physical–dynamical mechanism outlined above, directly attributable to changing in the land cover within the pair of simulations, is the key factor not only in determining the redistribution of convective rainfall, but also in the resulting regional decrease.

4. Sensitivity tests

In this section, the sensitivity of the results to various aspects of the model setup is explored. Using the default configuration (see section 2b) as the control, the July–August 1989 pair of simulations was repeated with three alternative model configurations. The first alternative used the Chen–Cotton (1983) radiative transfer scheme,

and the second used the Kuo convective parameterization. The third alternative used the default physics options, but at a 40-km grid spacing. Using both the default physics and grid spacing, three additional experiments were conducted to examine the impact of initial soil moisture and the distribution of SST. The first experiment used alternative initial soil moisture, the second an alternative SST distribution, and the third included both of these alternatives.

The factors explored in this analysis were chosen because they were thought to be of first-order importance to the nature of the model fields examined in this study (e.g., the surface energy budget and convective precipitation). However, these factors are by practical necessity a limited subset of those that could impact the results. Numerous other aspects of the model setup could potentially influence the results. For example, these simulations did not employ explicit cloud microphysics, because the resulting precipitation totals with use of a convective parameterization alone appeared adequate to

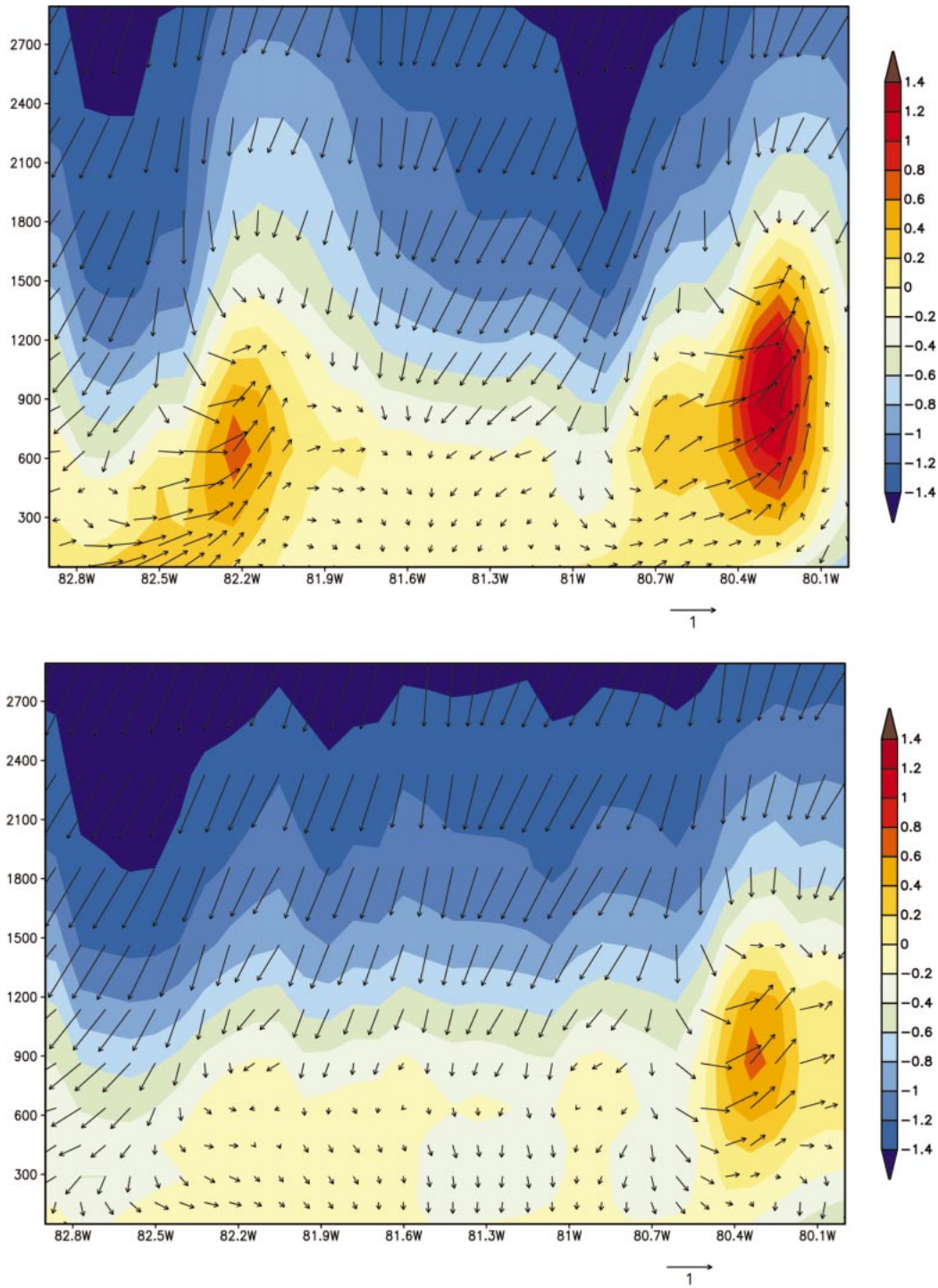


FIG. 18. Two-month average of the 1600 UTC u - w wind component (vectors are in m s^{-1} , but w component is multiplied by 100 for visual emphasis) and vertical velocity (cm s^{-1} ; color shaded) from the simulations for Jul-Aug 1989 with (top) pre-1900s land cover and (bottom) 1993 land use. The vertical cross section is the average of all possible cross sections from 26.5° to 28°N .

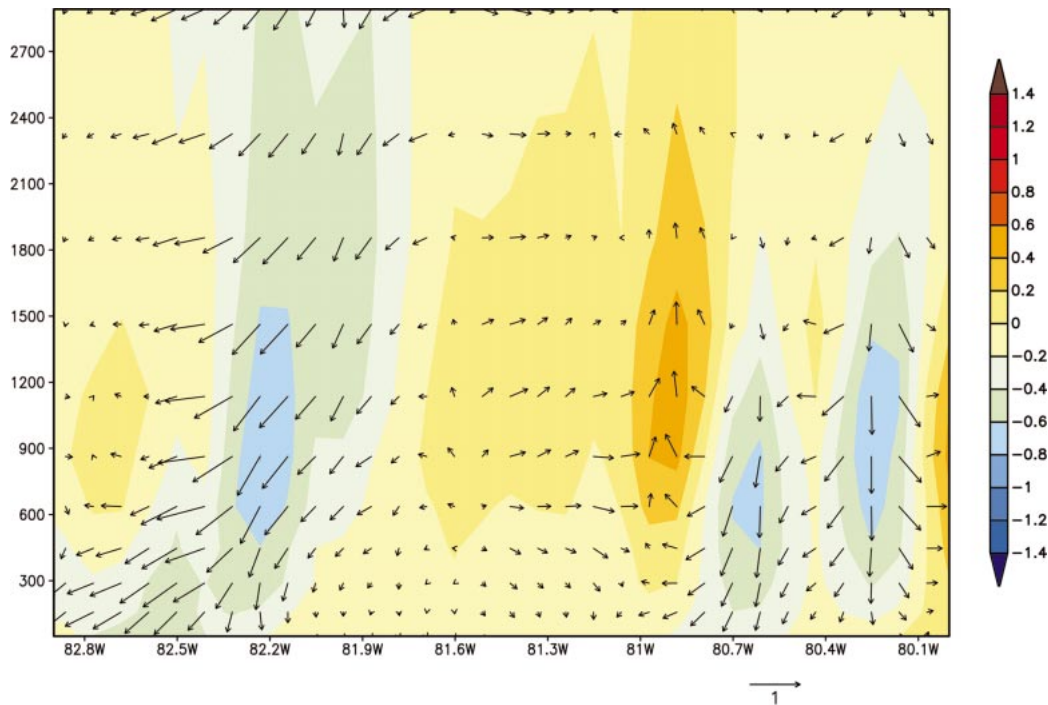


FIG. 19. Difference (1993 minus pre-1900 case) of the fields shown in Fig. 18.

capture the magnitude of the observed rainfall. For the sake of brevity, only the rainfall difference fields produced from the two land-cover scenarios within a given set of sensitivity simulations are shown (Fig. 20). In the case of experiments concerning soil moisture and SST, only the difference field wherein both factors are incorporated is provided. However, a histogram is provided that shows the grid-average rainfall (for both land-cover scenarios) for all four combinations of soil moisture and SST experiments (Fig. 21).

Much of the convective rainfall over the Florida peninsula during July and August is associated with circulations that are forced by spatially varying surface properties—particularly the sea breezes. Thus, it is reasonable to expect that the parameterized radiation, which provides the primary forcing for the surface sensible and latent heat fluxes, could have an impact on the nature of those circulations, and hence the distribution of convective rainfall. The Mahrer–Pielke (1977) scheme (the default) accounts for the presence of water vapor, but it does not explicitly account for cloud liquid water or ice in determining the radiative transfer. However, during the typical diurnal scenario, circulations such as the sea breezes are often well developed before the onset of significant convective cloudiness and rainfall. Thus, it is suggested that the Mahrer–Pielke scheme, which is desirable because of its computational efficiency, is adequate for the simulations presented in this study. Nevertheless, it is prudent to examine the impact of using an alternative, such as the Chen–Cotton scheme, that does incorporate the effects of cloud water

and ice. As Fig. 20a illustrates, the spatial distribution of the precipitation difference field is quite similar to the control field (Fig. 5, bottom). The axis of increase through the Kissimmee River valley is not as distinct as in the control case, but the general pattern of increase over the interior peninsula and decreases on adjacent sides is realized with the use of the Chen–Cotton scheme. The grid-average decrease is 18% of the pre-1900 total. The magnitude of this decrease is somewhat larger than the control, which was 11%. This result indicates that accounting for clouds in the radiative transfer has magnified the impact of land-cover change. A detailed investigation of the possible reasons for the difference with the control is not the primary focus of this study. The point emphasized here is that, even with an alternative radiation treatment, the difference realized because of changing the land cover is qualitatively similar and quantitatively not far removed.

Figure 20b shows that the model configuration with the Kuo scheme produced significantly less precipitation when the 1993 land cover is employed. The grid-average decrease is 13% of the pre-1900 total, which is very close to the percentage decrease in the control. The percentage change is very similar, despite the fact that, as with the 1973 results shown in Pielke et al. (1999), the overall Kuo scheme totals for both land-cover cases were significantly less than those produced by the Kain–Fritsch configuration (maps of these totals are not shown here). For the pre-1900 land-cover case, the Kuo configuration resulted in a grid-average total of 198 mm, whereas for the 1993 case this total was 173 mm. The

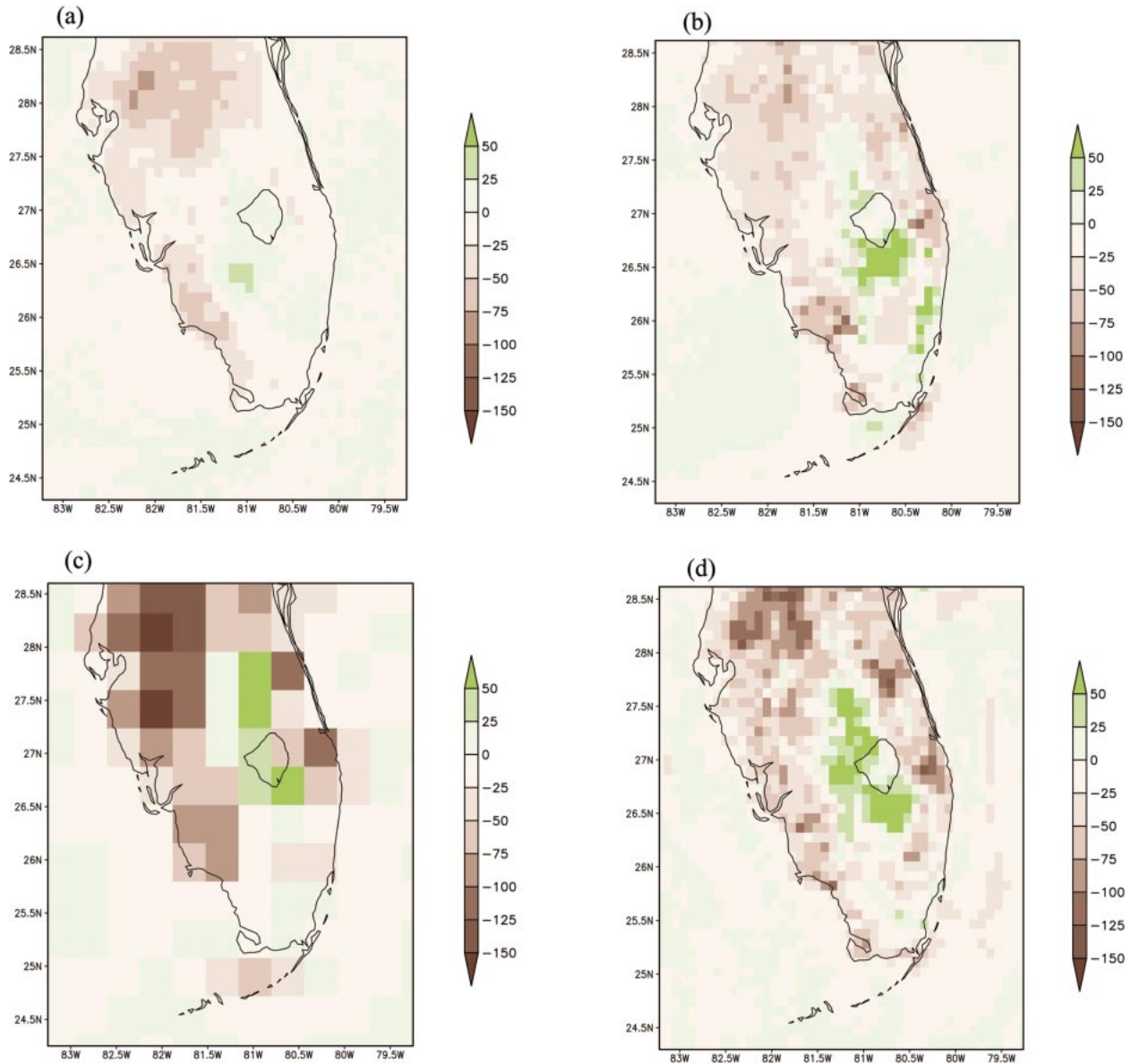


FIG. 20. Difference field of accumulated precipitation (mm; 1993 minus pre-1900) from the simulations for Jul–Aug 1989 incorporating (a) the Chen–Cotton radiation scheme, (b) the Kuo convection scheme, (c) default physics at 40-km grid spacing, and (d) default physics, with weekly observed SST and VIC model initial soil moisture.

Kain–Fritsch scheme yielded 342 mm for the pre-1900 case and 305 for the 1993 case.

The horizontal grid spacing would be expected to have significant impacts on the results, regardless of the choices for various physical parameterizations. Moreover, the effects of the physical parameterizations on the grid scale tendencies are themselves strongly influenced by the horizontal grid spacing. In other words, the horizontal grid spacing and the options selected for the physical parameterizations cannot be considered as mutually exclusive categories in this sensitivity analysis because these factors are inherently interactive. This is true especially for the convective parameterization, be-

cause convective schemes are designed precisely for a particular range of grid spacing. Figure 20c shows that the results at 40 km, produced with the same physics options used in the control (Kain–Fritsch convection and Mahrer–Pielke radiation), yielded a similar pattern of change in convective rainfall when the pre-1900 land cover is replaced with the 1993 dataset. The percentage decrease, 9.5%, is close to the 11% noted for the control (10 km) case. The overall precipitation totals in both land-cover scenarios (not shown here) were considerably larger than for the 10-km cases, with local maximums exceeding 700 mm. The 10-km maximums were less than 450 mm (see Fig. 5, top two panels). This

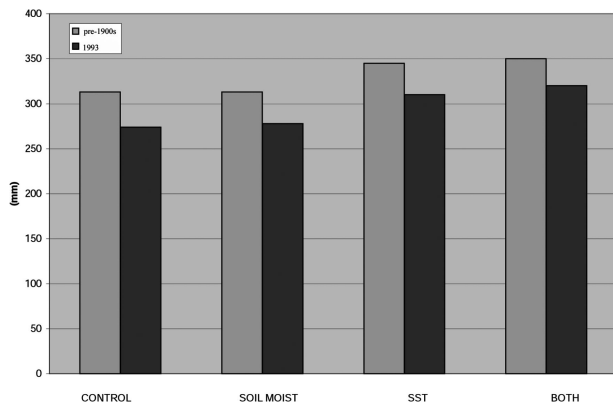


FIG. 21. Histogram of grid-average accumulated rainfall (mm) of all possible combinations of SST and soil moisture sensitivity experiments with the Jul–Aug 1989 simulations for both land-cover scenarios.

means that the 10-km totals were in much closer agreement with the observed magnitudes (Fig. 3). Regardless, the important point emphasized here again is that the difference in precipitation totals between land-cover scenarios *at either resolution* is qualitatively and quantitatively (as a percentage change of the pre-1900 total) similar. This result suggests that the impact of changing the land cover is consistent, regardless of the model grid spacing. Here, this sensitivity was evaluated by examining the results from a model configuration with larger grid spacing than that assigned to the control. However, it is acknowledged that the results could also differ if the model grid increment were smaller than the 10-km control value. At grid increment sizes much below this value, where the model setup could be configured to resolve convection explicitly, the representation of circulations such as the sea breezes could change markedly (and highly nonlinearly) with small changes in grid spacing (Weaver et al. 2002). Here, however, the analysis has been purposely designed to provide results that correspond to a range of grid increments over which the Kain–Fritsch convective parameterization is typically applied.

Other aspects of the model setup besides the physical parameterizations and grid spacing could have similar and even greater impacts on the results of changing the land cover. Two variables in particular that are believed to have a significant impact on warm season convective rainfall in regional/seasonal climate modeling simulations are the specification of SST and initial soil moisture (Walker and Rowntree 1977; Mintz 1984; Atlas et al. 1993; Paegle et al. 1996; Fennessey and Shukla 1999). Using the July–August 1989 simulations as the control, a factorial set of experiments was undertaken (i.e., one addressing initial soil moisture, a second addressing the specification of SST on the regional mode grid, and a third addressing both factors in combination). Note that any effects of SST anomalies at remote locations, such as the equatorial Pacific, are realized

through the lateral boundary conditions as specified directly by the NCEP–NCAR reanalysis data. As such, the question of interest here concerns SSTs in the adjacent coastal waters of the RAMS domain and what impact their specification may have on the resulting distribution of convective precipitation on the regional model grid.

In the control simulations, the SSTs were defined based on monthly climatology, as described in section 2b. For the sensitivity studies, a weekly observed dataset from NCEP was used (Reynolds and Smith 1994). For the period July–August 1989, the 2-month average of the weekly observed fields is quite different from the corresponding monthly climatological data (Fig. 22). Note that the Gulf Stream is locally several degrees warmer. In addition, the climatological dataset, which combines many years of multiple observations, is spatially smoother than the weekly data, which are based on a coarse-grid objective analysis of limited observational data.

For the sensitivity tests involving initial soil moisture, the alternative initialization was derived from the dataset produced by the University of Washington with the Variable Infiltration Capacity (VIC) model [see Maurer et al. (2002) for a description of both the VIC model and the production of this dataset]. These data are based on the execution of the VIC hydrologic model, as forced with observed rainfall and other observed and derived fields required to provide forcing to the VIC soil hydrologic budget. To initialize RAMS soil moisture, VIC soil moisture was first converted to a percent saturation value corresponding to VIC soil properties. These percentage values were in turn converted to volumetric water content values for RAMS that correspond to the spatially distributed hydraulic properties provided by the FAO soil properties dataset (see section 2b). The 2-m vertical average value derived from VIC was assigned to all vertical levels of a RAMS/LEAF-2 soil column. Figure 23 shows the initial soil moisture for both the pre-1900 and 1993 land-cover scenarios. Note that the initial field is different for the two different land-cover cases because of the imposed saturation condition for swamp and marsh classes. The spatial distribution of these classes is different between the two land-cover datasets. Also note the large area of the Everglades that has volumetric water contents greater than 0.8. In the FAO soil type database, these areas are designated as organic types, which have a very large porosity (i.e., soil moisture saturation value). As discussed by Baker et al. (2001), these properties of the land surface of the Florida peninsula, and their interplay with soil moisture, could have substantial impacts on the nature of local circulations and the interplay of those circulations with the sea breezes.

Figure 21 provides the grid-average rainfall (both land-cover scenarios) for the factorial set of SST and soil moisture experiments. There are substantial differences in the absolute totals among the experiments.

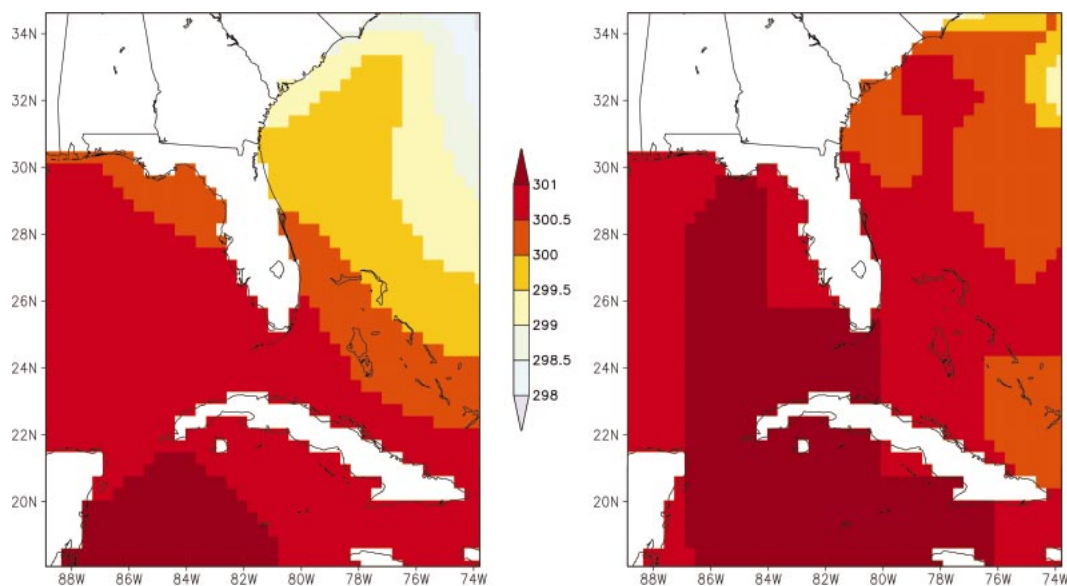


FIG. 22. Jul–Aug average SST (K) for the weekly observed NCEP data from (left) 1989 and (right) the monthly climatological dataset.

However, the difference between land-cover scenarios *within a given sensitivity experiment* is consistent, lending further credence to the robustness of the impact of land-cover change on convective precipitation in these simulations. The decrease relative to the pre-1900 totals for all four experiments is in the range of 10% to 12%, which is identical to the range for all three periods simulated with the control setup. The spatial nature of the difference field for the experiment incorporating both factors (Fig. 20d) is consistent with the results presented above, with substantial increases in precipitation directly over the Kissimmee River basin and decreases along the adjacent sea-breeze fronts.

5. Comparison of model results with observed trends

In light of the expanded scope of the simulations shown in this present study, it is also of interest to revisit and expand upon the earlier observational data analysis provided by Pielke et al. (1999). In the previous work, time series of July–August accumulated rainfall and mean shelter-level temperature observations from Everglades City, Belle Glade, and Fort Lauderdale, Florida, were presented. Here, data from these and several more stations (see Fig. 24 for all station locations) were compiled to provide long-term, regional-average time series. Furthermore, the July–August regional-mean time series of daily maximum and minimum temperature are provided in lieu of the single mean observed value shown in the previous study.

Data for Arcadia, Belle Glade, Everglades City, and Fort Lauderdale, Florida, through 2000 were obtained from the National Oceanic and Atmospheric Administration

(NOAA) National Climatic Data Center (NCDC) United States Historical Climatology Network (USHCN) Serial 2000 Temperature and Precipitation Dataset. The analysis of rainfall data from these stations was based on the unadjusted area-edited (i.e., original or “raw”) USHCN monthly total precipitation data. These totals were screened by NCDC to flag outliers, defined as three standard deviations beyond the mean for the period of record. Temperature data were subjected to NCDC USHCN 2000 quality assurance procedures. Specifically, these data are from the “area-edited, time of observation” data that have been adjusted for maximum and minimum system bias and station moves, with estimated values for missing and outlier data. However, these data were not subjected to the NCDC adjustment for urban heat island effects. The NCDC data for all July and August periods were nearly complete, with the few instances of missing data estimated from nearby station records. The Florida Climate Center provided the data for the remaining stations shown in Fig. 24, with the exception of rainfall data for HGS1, which was provided by the South Florida Water Management District.

Several limitations should be considered when comparing this observational data with the model results. First, the observations are point specific, whereas the model values represent an average over the finite area covered by the corresponding 10 km × 10 km grid cell. Thus, it is possible that an observation at a particular point, otherwise free of error, will differ significantly from the corresponding model grid value, which itself could accurately portray the average over the grid cell area. In order to minimize this source of uncertainty, observational data were spatially averaged. The resulting composite time series were then used for comparison

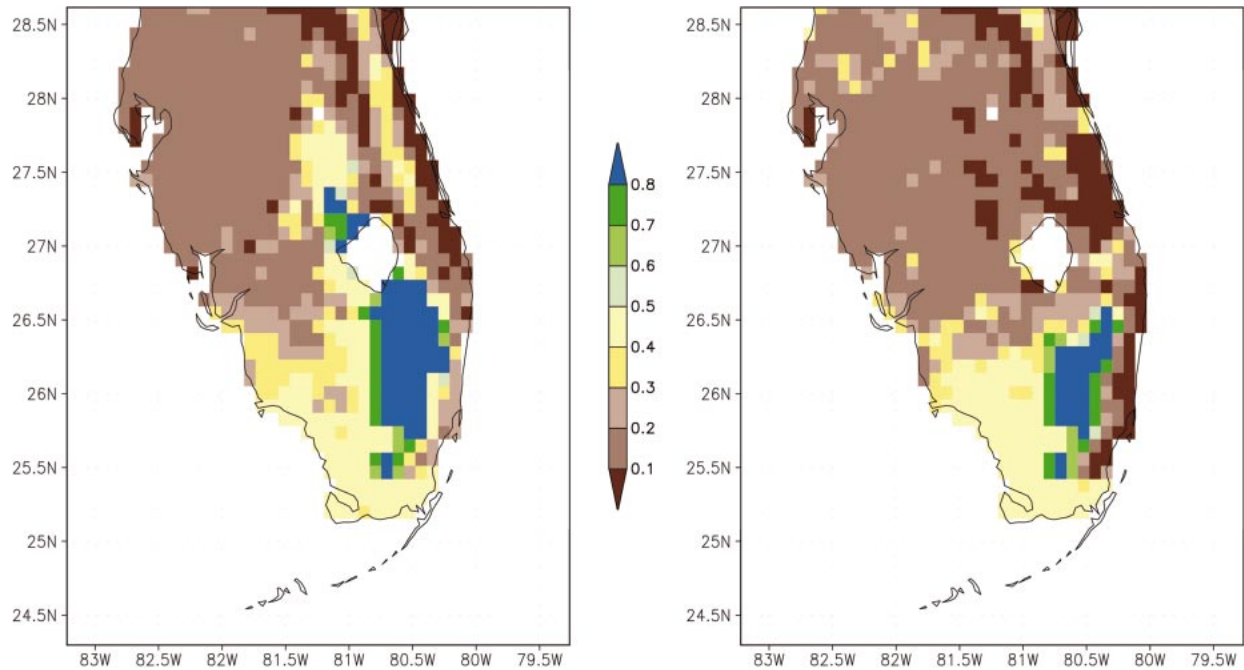


FIG. 23. Initial soil moisture ($\text{m}^3 \text{m}^{-3}$) as derived from the VIC model valid for 1 Jul 1989 for the (left) pre-1900 land cover and (right) 1993 land use.

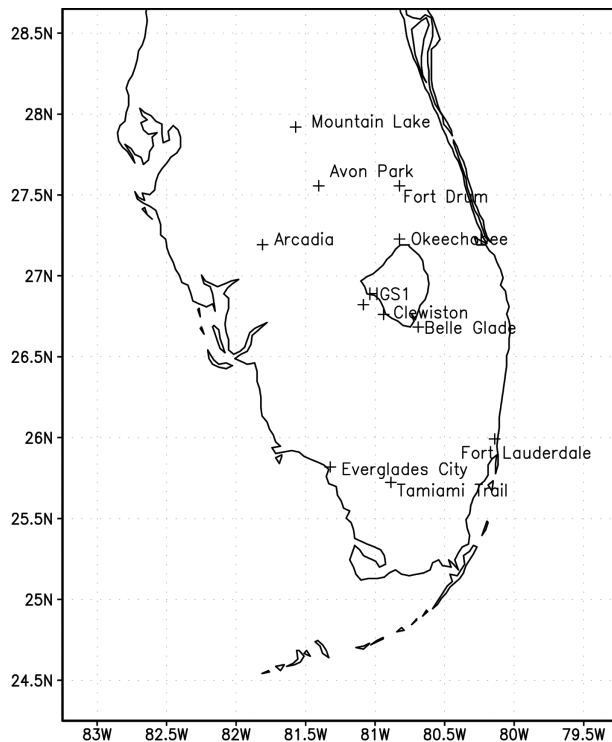


FIG. 24. Locations of observation stations used to compile regional-average long-term time series.

with model domain-average data. Second, instrument platforms for a given station designation were periodically relocated (often by as much as several kilometers) during the long-term period of interest. It is plausible that such relocations could have a marked impact on the observed trend for a particular station. Third, the number of stations with long-term records is rather limited, thereby constraining the sample size used to construct long-term time series of regional average data. Finally, observations of all three variables of interest were not always available from a particular station for all times during the long-term period of interest.

It must also be recognized that long-term time series of July–August observations and model simulations for *only three* July–August periods of interest that employ two land-cover datasets that were constructed to represent the long-term change do not constitute two otherwise identical statistical samples. The valid times for the two different land-cover scenarios used within a given pair of simulations correspond roughly to the end points of the long-term observational time series provided, so different results within a pair of simulations may provide physical insight into the possible impact of long-term land-cover change regional climate trends. However, a statistically rigorous comparison with corresponding observations would require data from model simulations for every July–August period used to construct the observational time series. Furthermore, each of these simulations would need to employ a land-cover database valid for each of the individual July–August periods in the time series. Such datasets are not available, rendering this task impossible at this time.

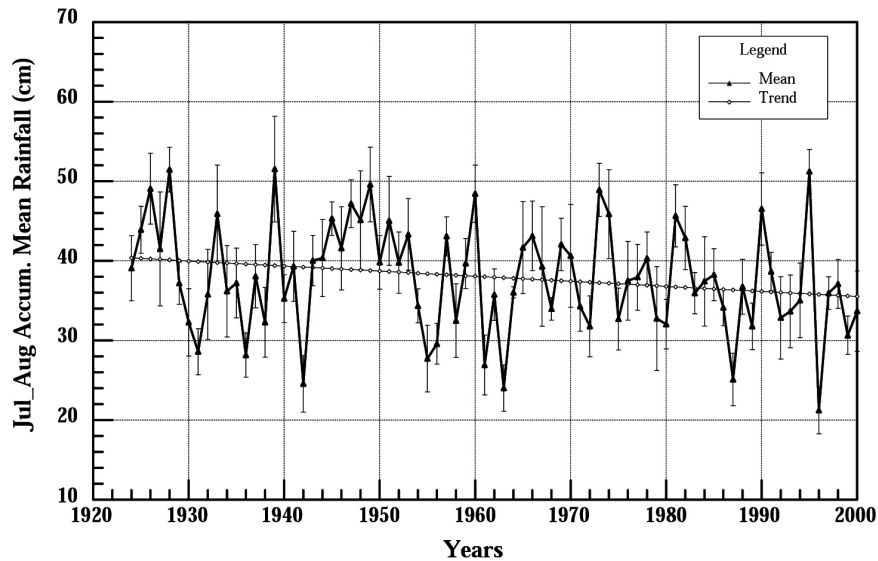


FIG. 25. Regional-average time series of accumulated convective rainfall (cm) from 1924 to 2000, with corresponding trend based on linear regression of all Jul–Aug regional average amounts. The vertical bars overlain on the raw time series indicate the value of the standard error of the Jul–Aug regional mean.

The time series of the regional-average July–August rainfall for the period 1924–2000 is shown in Fig. 25 (insufficient data prevented a start date prior to 1924), along with a trend based on a linear regression that incorporates all years in the sample. The linear trend has a slope of -0.064 , with a total decrease of 5 cm, or 12%, over the period of record. This is consistent with the percentage decrease of the domain-average convective precipitation from the model results. The standard error bars overlain on the raw time series indicate an appreciable spread among the individual station totals for a given July–August period, but the error value is typically less than 25% of the regional mean for its period. Eight out of ten of the time series for the individual observation locations (not shown here) used to construct the regional-mean precipitation time series exhibited a decreasing trend in July–August precipitation during their respective observational period of record. Station spacing and location, along with the considerations discussed above, preclude a detailed comparison of these individual trends with the spatial character of differences within land-cover pairs of simulations. In particular, the lack of long-term records for stations in the heart of the Kissimmee River valley prohibits an analysis of whether this area has actually seen an *increase* in rainfall. Prior to land-cover conversion, these areas were inaccessible wetlands and largely devoid of meteorological observation sites.

Lack of available long-term records for temperature observations at all the sites shown in Fig. 24 prohibited a start date prior to 1948 for the regional-mean time series of maximum and minimum temperature (Fig. 26). However, clear trends emerge in the available data, as the time series for both the July–August daily maximum

and minimum temperature indicate warming. The trend from linear regression has a slope of 0.011° (0.009°) yr^{-1} , with a magnitude of 0.57°C (0.46°C) for the maximum (minimum) temperature increase over the period 1948–2000. The maximum temperature trend is in reasonable agreement with the model domain-average increase of 0.31°C (Fig. 13) that occurs when the pre-1900 dataset is replaced with 1993 land use in the simulations. Recall, however, that the change in model minimum temperature indicated slight cooling (-0.26°C for the grid average; Fig. 14). This discrepancy could result from a number of factors, including model error or inadequate observational sampling of those areas with the greatest cooling in the model that are in the heart of the poorly sampled Kissimmee River valley. In the case of model minimum temperature, the vertical resolution in the lower levels and the parameterization of stable boundary layer processes could result in inadequate representation of shallow nocturnal circulations. In addition, the subgrid-scale variability of minimum temperature is potentially greater than that for the daytime maximum, because the latter typically is more spatially homogenized when the boundary layer is more mixed. Furthermore, shelter-level temperatures are not predicted explicitly by the model but are diagnosed using similarity theory (Monin and Obukhov 1954). Numerous factors in the similarity theory framework could introduce error in the estimates, and this error may not be consistent for stable versus unstable (i.e., daytime maximum and nighttime minimum) conditions. Subtle differences between the elevation of the observing platform and the model grid cell effective elevation may also result in diagnosis of a temperature value that is not at the exact elevation of the observation. This error

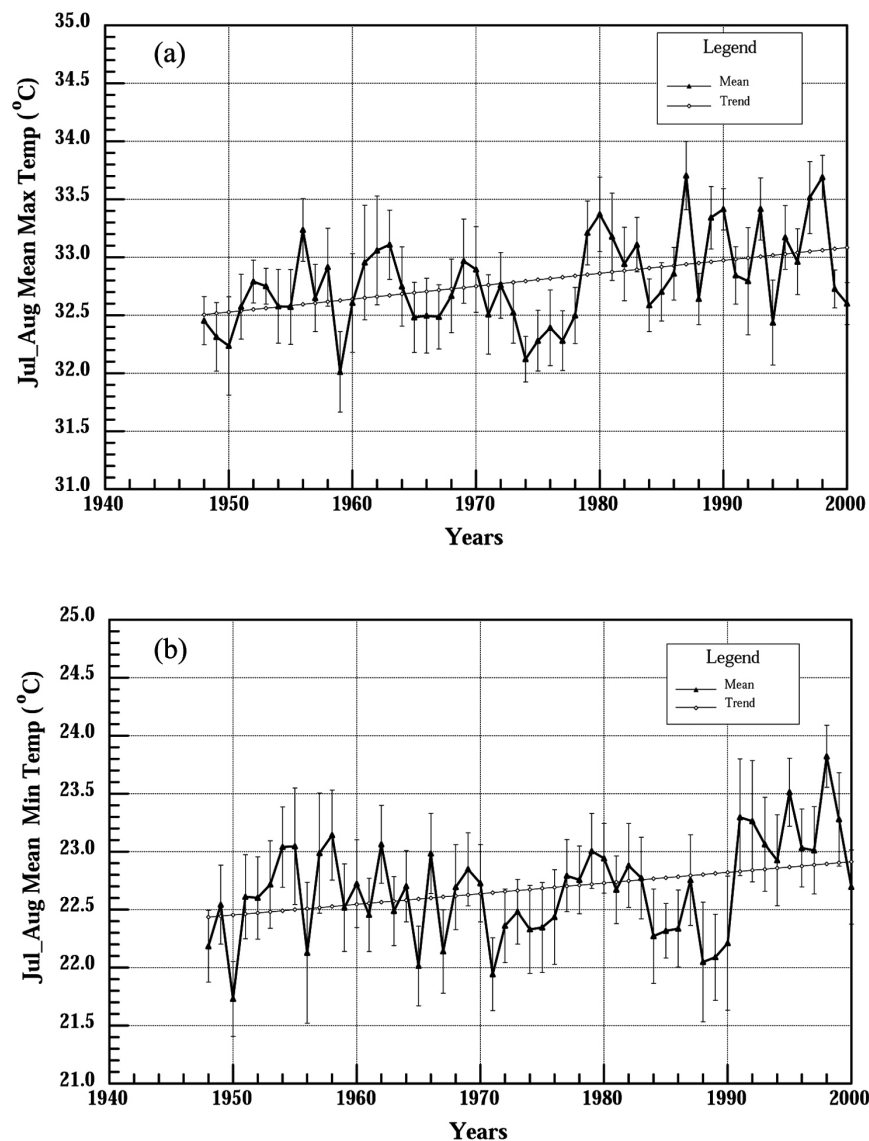


FIG. 26. Same as Fig. 25, except for daily (a) max and (b) min shelter-level temperature ($^{\circ}\text{C}$).

can be large when steep, surface-based thermal inversions are present, such as the time when the daily minimum temperature is observed. It must also be recognized that the observational time series could be indicative of a regional or larger-scale trend in nocturnal warming that is indeed real, and that it could be the result of factors independent of those addressed in this study.

6. Concluding remarks

Both anecdotal evidence and scientific investigations have led to the suggestion that the Florida peninsula witnessed increasing summertime maximum temperatures and decreasing warm season convective rainfall during the twentieth century. This study has expanded

upon the previous work of Pielke et al. (1999) by undertaking a more comprehensive set of numerical simulations with the RAMS model to further investigate the question of whether these trends can be attributed, at least in part, to land-cover change. The results of the simulations support the earlier findings that, in general, summertime maximum temperatures increased and convective rainfall decreased when natural vegetation was replaced with current land cover. When averaged over the model domain, the diurnal cycle was amplified, with higher afternoon maximum and lower nighttime minimum. This signature was especially apparent in areas of the interior peninsula that were drained of standing water and converted to agricultural land during the twentieth century. Over those areas, the model afternoon maximum temperatures warmed by as much as several

degrees because of land-cover change alone. Furthermore, changing the land cover to 1993 conditions resulted in a decrease in the grid-average convective rainfall.

The analysis presented in this paper is significantly more comprehensive than that provided by the previous study in examining the relationships among land-cover change, surface fluxes, the detailed character of surface-forced circulations, diurnal cycles of shelter-level temperature, and the spatial distribution and amount of convective rainfall. In particular, a physical–dynamical link between the land-cover change and the overall regional trend of decreasing rainfall is provided. In this present work, it has been shown that changes in the land surface directly impacted the structure and strength of the modeled sea-breeze circulations. In the pre-1900 land cover scenario, the minimum in sensible heat flux over the inundated floodplain of the Kissimmee River basin was associated with an outward-directed mesoscale flow that served to constructively reinforce the sea breezes. Changing the land surface to 1993 conditions effectively removed this feature, resulting in weakening of the upward branches of the sea-breeze circulations over areas immediately on either side of the Kissimmee basin, with a weakening of the compensating subsidence over the center of the basin itself. This change in the low-level wind field was associated with an increase in precipitation over the immediate interior of the peninsula, with general decreases elsewhere. When expressed as a spatial average over the model domain, the precipitation decreased by 10% to 12% of the pre-1900 total. The changes in both the spatial distribution and the grid-average percentage decrease were remarkably consistent among all three simulated periods. These differences within a given pair of simulations were also present when the simulations were repeated with a variety of sensitivity factors, despite varying magnitudes among the resulting rainfall totals. The consistency in the changes between land-cover scenarios among the various pairs of sensitivity experiments lends greater credence to the suggestion that anthropogenic land-cover changes could be responsible for significant changes in the warm season precipitation climatology of the Florida peninsula.

Limited observational data were analyzed to provide long-term regional trends during the period spanned by the two land-cover scenarios. The observed trends indicate warming of July–August daytime maximum temperature and decreased rainfall. However, the observational trend of nighttime minimum indicates warming, which is inconsistent with the model results. It is difficult to know whether this discrepancy results from model error and uncertainty, observational error and uncertainty, or some combination of these factors.

These results could have important implications for land use and water resource management interests in south Florida, including the ongoing efforts to preserve and protect the Everglades ecosystem. The findings pre-

sented in this paper imply that restoration of a more natural flow regime and the resulting land-cover changes would alter the distribution of typical low-level wind patterns and associated convective rainfall, as well as change the surface diurnal cycle of shelter-level temperature. Furthermore, these results provide additional evidence to support the suggestion that land-cover change should be considered as a potentially significant factor in studies that provide information regarding climate trends.

Acknowledgments. We thank David Zierden, Jim O'Brien, and Melissa Griffin of the Florida Climate Center for their assistance in providing daily and monthly rainfall and temperature data for selected surface weather stations in Florida and for their recommendations concerning anomalously wet, average, and dry rainfall years in south Florida. The contributions of John W. Jones, Tom Smith III, and Tom Cronin of the U.S. Geological Survey and Jim Irons of the NASA Goddard Space Flight Center are appreciated. Adriana Beltran and Chris Castro are credited for the implementation of the Kain–Fritsch scheme in the RAMS model. Bob Walcko provided invaluable help with incorporating the USGS vegetation datasets into the RAMS model. Funding for this research was provided by USGS Grant 1434-CR-97-AG-00025, Task 7, and the USGS Geographic Research Applications Prospectus Activity.

REFERENCES

- Anthes, R. A., 1984: Enhancement of convective precipitation by mesoscale variations in vegetative covering in semiarid regions. *J. Climate Appl. Meteor.*, **23**, 541–554.
- Atlas, R., N. Wolfson, and J. Terry, 1993: The effect of SST and soil moisture anomalies on GLA model simulations of the 1988 U.S. summer drought. *J. Climate*, **6**, 2034–2048.
- Baker, R. D., B. H. Lynn, A. Boone, W.-K. Toa, and J. Simpson, 2001: The influence of soil moisture, coastline curvature, and land-breeze circulations on sea-breeze initiated precipitation. *J. Hydrometeorol.*, **2**, 193–211.
- Boyle, R. H., and R. M. Mechem, 1982: Anatomy of a man-made drought. *Sports Illustrated*, **56**, 46–54.
- Byers, H. R., and H. R. Rodebush, 1948: Causes of thunderstorms in the Florida peninsula. *J. Meteor.*, **5**, 275–285.
- Chen, C., and W. R. Cotton, 1983: A one-dimensional simulation of the stratocumulus-capped mixed layer. *Bound.-Layer Meteorol.*, **25**, 289–321.
- Costanza, R., 1975: The spatial distribution of land use subsystems, incoming energy and energy use in south Florida from 1900 to 1973. M.S. thesis, Dept. of Architecture, University of Florida. [Available from Dept. of Architecture, University of Florida, P.O. Box 115702, Gainesville, FL 32611.]
- , 1979: Embodied energy basis for economic-ecologic systems. Ph.D. dissertation, University of Florida, 253 pp. [Available from Dept. of Architecture, University of Florida, P.O. Box 115702, Gainesville, FL 32611.]
- Cressman, G., 1959: An operational analysis system. *Mon. Wea. Rev.*, **87**, 367–374.
- Dalu, G. A., and R. A. Pielke, 1993: Vertical heat fluxes generated by mesoscale atmospheric flow induced by thermal inhomogeneities in the PBL. *J. Atmos. Sci.*, **50**, 919–926.
- Davis, J. H., Jr., 1943: The natural features of southern Florida. *Geological Bulletin*, No. 25, Florida Geological Survey, 130–215.

- FAO, 1997: Digital soil map of the world and derived soil properties. Version 3.5. FAO.
- Fennessy, M. J., and J. Shukla, 1999: Impact of initial soil wetness of seasonal atmospheric prediction. *J. Climate*, **12**, 3167–3180.
- Gannon, P. T., and T. E. Warner, 1990: Drought over south Florida: Mesoscale or synoptic scale? Preprints, *Eighth Conf. on Hydro-meteorology*, Kananaskis Park, AB, Canada, Amer. Meteor. Soc., 3–6.
- Kain, J. S., and J. M. Fritsch, 1993: Convective parameterization for mesoscale models: The Kain–Fritsch scheme. *The Representation of Cumulus Convection in Numerical Models*, Meteor. Monogr., No. 46, Amer. Meteor. Soc., 165–170.
- Kalnay, E., and Coauthors, 1996: The NCEP/NCAR 40-Year Reanalysis Project. *Bull. Amer. Meteor. Soc.*, **77**, 437–471.
- Küchler, A. W., 1964: Potential natural vegetation of the conterminous United States. American Geophysical Society Special Publ. 36, 156 pp.
- Kuo, H. L., 1974: Further studies of the parameterization of the influence of cumulus convection on large-scale flow. *J. Atmos. Sci.*, **31**, 1232–1240.
- Kushlan, J. A., 1990: Freshwater marshes. *The Ecosystems of Florida*, R. L. Meyers and J. J. Ewel, Eds., University of Central Florida Press, 324–363.
- Landers, J. L., and W. D. Boyer, 1999: An old-growth definition for upland longleaf and south Florida slash pine forests, woodlands, and savannas. Southern Research Station, Forest Service. General Tech. Rep. SRS-29, U.S. Dept. of Agriculture, Asheville, NC, 15 pp.
- Light, S. S., and J. W. Dineen, 1994: Water control in the Everglades: A historical perspective. *The Everglades: The Ecosystem and Its Restoration*, S. M. Davis and J. C. Ogden, Eds., St. Lucie Press, 47–84.
- Louis, J. F., 1979: Parametric model of vertical eddy fluxes in the atmosphere. *Bound.-Layer Meteor.*, **17**, 187–202.
- Mahrer, Y., and R. A. Pielke, 1977: A numerical study of the airflow over irregular terrain. *Beitr. Phys. Atmos.*, **50**, 98–113.
- Maurer, E. P., A. W. Wood, J. C. Adam, D. P. Lettenmaier, and B. Nijssen, 2002: A long-term hydrologically based dataset of land surface fluxes and states for the conterminous United States. *J. Climate*, **15**, 3237–3251.
- McVoy, C., 1996: Comparison of the South Florida Natural System Model with pre-canal Everglades hydrology estimated from historical sources. U.S. Geological Survey Fact Sheet FS-187-96, 2 pp. [Available online at <http://sflwww.er.usgs.gov/publications/fs/187-96/>]
- , W. A. Park, and J. Obeysekera, 2003: Landscapes and hydrology of the Everglades, circa 1850. U.S. Geological Survey Open File Report.
- Michaels, P. J., R. A. Pielke, J. S. McQueen, and D. E. Sappington, 1987: Composite climatology of Florida summer thunderstorms. *Mon. Wea. Rev.*, **115**, 2781–2791.
- Mintz, Y., 1984: The sensitivity of numerically simulated climates to land-surface conditions. *The Global Climate*, J. Houghton, Ed., Cambridge University Press, 79–105.
- Monin, A. S., and A. M. Obukhov, 1954: Basic laws of turbulent mixing in the atmosphere near the ground. *Tr. Geofiz. Inst. Akad. Nauk SSSR*, **24**, 1963–1987.
- Paegle, J., K. C. Mo, and J. Nogués-Paegle, 1996: Dependence of simulated precipitation on surface evaporation during the 1993 United States summer floods. *Mon. Wea. Rev.*, **124**, 345–361.
- Pearlstine, L. G., S. E. Smith, L. Brandt, C. Allen, W. Kitchens, and J. Stenberg, 2002: Assessing statewide biodiversity in the Florida GAP Analysis Project. *J. Environ. Manage.*, **66**, 127–144.
- Pielke, R. A., 1974: A three-dimensional numerical model of the sea breezes over south Florida. *Mon. Wea. Rev.*, **102**, 115–139.
- , 2001: Influence of the spatial distribution of vegetation and soils on the prediction of cumulus convective rainfall. *Rev. Geophys.*, **39**, 151–177.
- , and W. R. Cotton, 1977: A mesoscale analysis over south Florida for a high rainfall event. *Mon. Wea. Rev.*, **105**, 343–362.
- , and Coauthors, 1992: A comprehensive meteorological modeling system—RAMS. *Meteor. Atmos. Phys.*, **49**, 69–91.
- , R. L. Walko, L. T. Steyaert, P. L. Vidale, G. E. Liston, W. A. Lyons, and T. N. Chase, 1999: The influence of anthropogenic landscape changes on weather in south Florida. *Mon. Wea. Rev.*, **127**, 1663–1673.
- Reynolds, R. W., and T. M. Smith, 1994: Improved global sea surface temperature analyses using optimum interpolation. *J. Climate*, **7**, 929–948.
- Schmidt, N., E. K. Lipp, J. B. Rose, and M. E. Luther, 2001: ENSO influences on seasonal rainfall and river discharge in Florida. *J. Climate*, **14**, 615–628.
- Segal, M., and R. W. Arritt, 1992: Non-classical mesoscale circulations caused by surface sensible heat flux gradients. *Bull. Amer. Meteor. Soc.*, **73**, 1593–1604.
- Simpson, J. E., 1994: *Sea Breeze and Local Winds*. Cambridge University Press, 234 pp.
- Smagorinsky, J., 1963: General circulation experiments with the primitive equations. Part I: The basic experiment. *Mon. Wea. Rev.*, **91**, 99–164.
- Tripoli, G. J., and W. R. Cotton, 1982: The Colorado State University three-dimensional cloud/mesoscale model—1982. Part I: General theoretical framework and sensitivity experiments. *J. Rech. Atmos.*, **16**, 185–219.
- Vogelmann, J. E., T. L. Sohl, P. V. Campbell, and D. M. Shaw, 1998: Regional land cover characterization using Landsat Thematic Mapper data and ancillary data sources. *Environ. Monit. Assess.*, **51**, 415–428.
- , S. M. Howard, L. M. Yang, C. R. Larson, B. K. Wylie, and N. Van Driel, 2001: Completion of the 1990s National Land Cover Dataset for the conterminous United States from Landsat Thematic Mapper Data and ancillary data sources. *Photogramm. Eng. Remote Sens.*, **67**, 650–662.
- Walker, J., and P. R. Rowntree, 1977: The effect of soil moisture on circulation and rainfall in a tropical model. *Quart. J. Roy. Meteor. Soc.*, **103**, 29–46.
- Walko, R. L., and Coauthors, 2000: Coupled atmosphere–biophysics–hydrology models for environmental modeling. *J. Appl. Meteor.*, **39**, 931–944.
- Weaver, C. P., and R. Avissar, 2001: Atmospheric disturbances caused by human modification of the landscape. *Bull. Amer. Meteor. Soc.*, **82**, 269–282.
- , S. Baidya, and R. Avissar, 2002: Sensitivity of simulated mesoscale atmospheric circulations resulting from landscape heterogeneity to aspects of model configuration. *J. Geophys. Res.*, **107**, 1–21.
- Wetzel, P. I., 1990: A simple parcel method for prediction of cumulus onset and area-averaged cloud amount over heterogeneous land surfaces. *J. Appl. Meteor.*, **29**, 516–523.
- Willard, D. A., L. M. Weimer, and W. L. Riegel, 2001: Pollen assemblages as paleoenvironmental proxies in the Florida Everglades. *Rev. Palaeobot. Palynol.*, **113**, 213–235.